AD-A140 891 ROTATING ARM EXPERIMENT FOR AN EXTENDED STRUT SWATH (SMALL WATERPLANE ARE..(U) DAVID W TAYLOR NAVAL SHIP RESEARCH AND DEVELOPMENT CENTER BET.. C J HART ET AL. 1/1

UNCLASSIFIED SEP 83 DTNSRDC/SPD-0698-03 F/G 13/10 NL

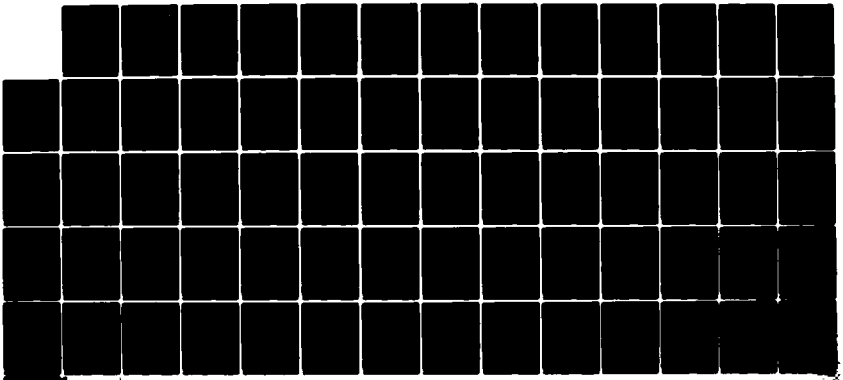

END
DATE FILMED
DTIC

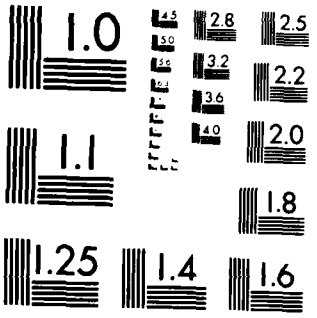

MICROCOPY RESOLUTION TEST CHART
NATIONAL BUREAU OF STANDARDS-1963-A

(12)

DAVID W. TAYLOR NAVAL SHIP RESEARCH AND DEVELOPMENT CENTER

Bethesda, Maryland 20084

ROTATING ARM EXPERIMENT FOR AN EXTENDED STRUT SWATH SHIP AS REPRESENTED BY THE SWATH-6E

CHRISTOPHER J. HART

R. THOMAS WATERS

JAMES HICKOK

APPROVED FOR PUBLIC RELEASE

DISTRIBUTION UNLIMITED

SHIP PERFORMANCE DEPARTMENT

SEPTEMBER 1983

DTNSRDC SPD-0698-03

AD-A140 891

DTIC FILE COPY

DTIC

NDW-DTNSRDC 5602/30 (2-80)
(supersedes 3960/46)

84 05 08 01

MAJOR DTNSRDC ORGANIZATIONAL COMPONENTS

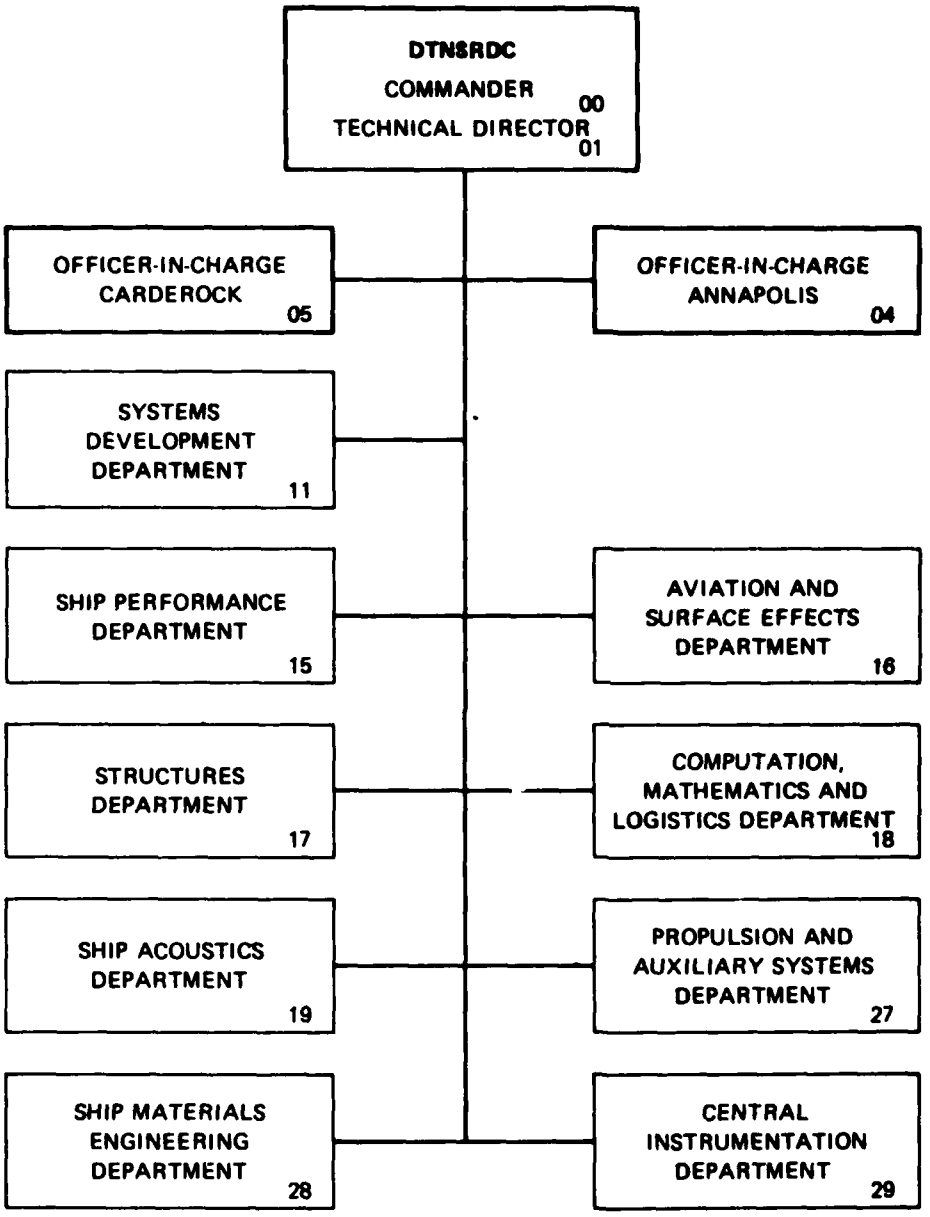

GPO 666 993

UNCLASSIFIED

SECURITY CLASSIFICATION OF THIS PAGE (When Date Entered)

REPORT DOCUMENTATION PAGE		READ INSTRUCTIONS BEFORE COMPLETING FORM
1. REPORT NUMBER DTNSRDC/SPD-0698-03	2. GOVT ACCESSION NO. AD-A140 891	3. RECIPIENT'S CATALOG NUMBER
4. TITLE (and Subtitle) Rotating Arm Experiment for an Extended Strut SWATH Ship as Represented by the SWATH-6E		5. TYPE OF REPORT & PERIOD COVERED Final 6. PERFORMING ORG. REPORT NUMBER
7. AUTHOR(s) Christopher J. Hart, R. Thomas Waters and James Hickok		8. CONTRACT OR GRANT NUMBER(s)
9. PERFORMING ORGANIZATION NAME AND ADDRESS David Taylor Naval Ship R&D Center Bethesda, Maryland 20084		10. PROGRAM ELEMENT, PROJECT, TASK AREA & WORK UNIT NUMBERS Ship, Subs and Boats Block Program Work unit No. 1-1506-102
11. CONTROLLING OFFICE NAME AND ADDRESS Naval Sea Systems Command Washington, DC 20362		12. REPORT DATE September, 1983 13. NUMBER OF PAGES
14. MONITORING AGENCY NAME & ADDRESS(if different from Controlling Office)		15. SECURITY CLASS. (of this report) Unclassified 15a. DECLASSIFICATION/DOWNGRADING SCHEDULE

16. DISTRIBUTION STATEMENT (of this Report)

Distribution Unlimited

17. DISTRIBUTION STATEMENT (of the abstract entered in Block 20, if different from Report)

18. SUPPLEMENTARY NOTES

19. KEY WORDS (Continue on reverse side if necessary and identify by block number)

SWATH
Maneuvering
Rotating Arm Experiments

20. ABSTRACT (Continue on reverse side if necessary and identify by block number)

This report contains the results of model scale experiments on the horizontal plane characteristics of an extended strut Small Waterplane Area Twin Hull (SWATH) ship. Experiments were conducted in the Rotating Arm Facility of the David Taylor Naval Ship Research and Development Center (DTNSRDC). Speed, drift angle, roll angle, yaw rate, and rudder deflection angle were varied at two drafts. Nondimensional derivatives are presented, and the the results provide a data base for prediction of the maneuvering performance of extended strut SWATH ships when compared to previous SWATH designs with spade and strut

DD FORM 1 JAN 73 1473 EDITION OF 1 NOV 65 IS OBSOLETE
S/N 0102-LF-014-6601

UNCLASSIFIED

SECURITY CLASSIFICATION OF THIS PAGE (When Date Entered)

-rudders of similar areas.

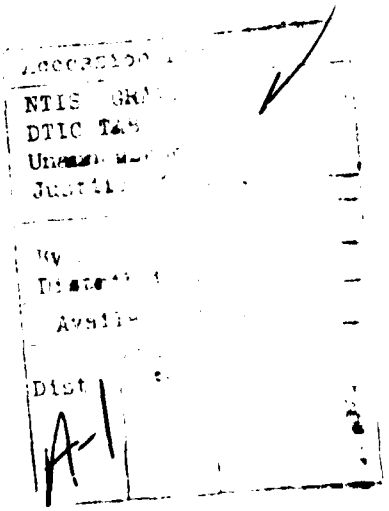

TABLE OF CONTENTS

LIST OF FIGURES

LIST OF FIGURES (Continued)

LIST OF FIGURES (Continuation)

LIST OF FIGURES (Continued)

LIST OF TABLES

NOTATION

Physical Quantities

ρ	Density of water
L	Characteristic length (hull length)
U	Linear velocity of vehicle
g	Gravitational acceleration constant
R	Radius of turn
β	Drift angle, positive nose-to-starboard
ϕ	Roll angle, positive starboard side down
ψ	Dimensional yaw rate
δ_r	Rudder angle, positive trailing-edge-to-port
$r' = L/R$	Nondimensional yaw rate
$v' = -\sin\beta$	Nondimensional sway velocity
c	Control surface chord length
a	Area
$AR = a/c^2$	Geometric aspect ratio
x_{CG}	Distance, reference point to center of gravity, + forward
x_{cg}	Distance, x_{CG} to center of fin area

Nondimensional Body Axis Forces and Moments

$$K' = \frac{K}{(\rho/2)\, L^3\, U^2} \qquad \text{roll moment}$$

$$M' = \frac{M}{(\rho/2)\, L^3\, U^2} \qquad \text{pitch moment}$$

$$N' = \frac{N}{(\rho/2)\, L^3\, U^2} \qquad \text{yaw moment}$$

$$X' = \frac{X}{(\rho/2)\, L^3\, U^2} \qquad \text{axial force}$$

$$Y' = \frac{Y}{(\rho/2)\, L^3\, U^2} \qquad \text{lateral force}$$

$$Z' = \frac{Z}{(\rho/2)\, L^3\, U^2} \qquad \text{vertical force}$$

NONDIMENSIONAL DERIVATIVES

$$N'_r = \left[\frac{\partial N'}{\partial r'}\right]_{r' = 0} \qquad N'_{vr} = \left[\frac{\partial N'}{\partial v' \partial r'}\right]_{v' \text{ and } r' = 0}$$

$$Y'_r = \left[\frac{\partial Y'}{\partial r'}\right]_{r' = 0} \qquad Y'_{vr} = \left[\frac{\partial Y'}{\partial v' \partial r'}\right]_{v' \text{ and } r' = 0}$$

$$K'_r = \left[\frac{\partial K'}{\partial r'}\right]_{r' = 0} \qquad K'_{vr} = \left[\frac{\partial K'}{\partial v' \partial r'}\right]_{v' \text{ and } r' = 0}$$

$$N'_v = \left[\frac{\partial N'}{\partial v'}\right]_{v' = 0} \qquad X'_{\delta_r \delta_r} = \left[\frac{\partial X'}{\partial \delta_r^2}\right]_{\delta_r = 0}$$

$$Y'_v = \left[\frac{\partial Y'}{\partial v'}\right]_{v' = 0} \qquad X'_{vv} = \left[\frac{\partial X'}{\partial v'^2}\right]_{v' = 0}$$

$$K'_v = \left[\frac{\partial K'}{\partial v'}\right]_{v' = 0} \qquad N'_\phi = \left[\frac{\partial N'}{\partial \phi}\right]_{\phi = 0}$$

$$N'_{\delta_r} = \left[\frac{\partial N'}{\partial \delta_r}\right]_{\delta_r = 0} \qquad Y'_\phi = \left[\frac{\partial Y'}{\partial \phi}\right]_{\phi = 0}$$

$$Y'_{\delta_r} = \left[\frac{\partial Y'}{\partial \delta_r}\right]_{\delta_r = 0} \qquad K'_\phi = \left[\frac{\partial K'}{\partial \phi}\right]_{\phi = 0}$$

$$K'_{\delta_r} = \left[\frac{\partial K'}{\partial \delta_r}\right]_{\delta_r = 0}$$

ABSTRACT

This report contains results of model scale experiments on the horizontal plane characteristics of an extended strut Small Waterplane Area Twin Hull (SWATH) ship. Experiments were conducted in the Rotating Arm Facility of the David Taylor Naval Ship Research and Development Center (DTNSRDC). Speed, drift angle, roll angle, yaw rate, and rudder deflection angle were varied at two drafts.

Nondimensional force and moment derivatives are presented, and the results provide a data base for prediction of the maneuvering performance of extended strut SWATH ships. The major conclusions obtained for an analysis of the empirical data are: the SWATH-6E design exhibits superior rudder performance at high speed, the extended strut design shows higher directional stability, and the SWATH-6E configuration shows greatly improved maneuvering performance at high speeds. When compared to previous SWATH designs with spade or strut rudders of similar areas.

ADMINISTRATIVE INFORMATION

This work funded by the Ships, Subs and Boats Block Program Element 62543, Task Area SF 421-350-200 SF, DTNSRDC work unit number 1-1506-102-11.

INTRODUCTION

An extensive rotating arm experimental program was conducted on a Small Waterplane Area Twin Hull (SWATH) ship represented by a 1/22.5 scale model (DTNSRDC MODEL 5337-E) designated SWATH-6E. These experiments were conducted to evaluate the horizontal plane characteristics of an extended strut SWATH ship, and to compare maneuvering performance with other SWATH hull configurations.

The SWATH-6E design is a modification of the SWATH-6A design (DTNSRDC MODEL 5337). The struts have been extended aft of the lower hulls allowing rudders to be placed in the propeller slip stream. The shape of the extended struts was developed by considering the powering, seakeeping and maneuvering characteristics of a series of candidate struts varying in waterplane area distribution.

The data from this experiment will be incorporated in a mathematical model that will be employed to predict turning capability, estimate rudder size, and design rudder systems for extended strut SWATH ships.

Experiments were conducted at four nondimensional yaw rates, varying from 0.103 to 0.418 on the Rotating Arm Facility at speeds corresponding to full scale speeds of 7, 10, 15, 20, 25 and 30 knots. The craft was held completely captive with respect to the towing rig throughout the experiment. Forces and moments were measured in all six degrees of freedom, and are defined under the coordinate system indicated in Figure 1. This report includes a description of the model, a discussion of test procedures, an analysis of the data, an interpretation of the results and pertinent conclusions.

DESCRIPTION OF MODEL

The geometric characteristics of the model are given in Table 1. The model used in this experiment was the 1/22.5 scale SWATH-6 series baseline model, fitted with new struts and rudders. These struts extend aft of the lower hulls, allowing the placement of the rudders in the propeller slip stream. The two SWATH-6 demi-hulls are connected by a plywood bridging structure, to which the gage assemblies were attached as shown in Figures 2 and 3. The SWATH-6E waterplane area, displacement, draft and hull spacing are the same as the other models of the SWATH-6 series. Details of the SWATH-6E modified struts and rudders are found in DTNSRDC Model drawings; reference numbers E15-3261-30, 31 and 32. The SWATH-6E rudders have an aspect ratio of 1.4 and a NACA 0021 section. The

hinge axis (rudder stock) is located at the quarter chord to provide semi-balanced rudders. For comparative purposes, the planform area of the SWATH-6E rudders corresponds to the SWATH-6A and 6B design draft rudder area. Rudder profile is shown in Figure 4. Rudder deflection angle was controlled with a hydraulic servo-actuator and had a maxmimum deflection angle of $\pm$ 30 degrees.

Model propulsion power was provided by two 5.4 horsepower D.C. motors housed one in each demi-hull, and DTNSRDC model propellers (numbers 4416 and 4417).

Turbulent flow on the model was induced by placing a series of turbulence stimulating studs (0.125 inches in diameter and 0.1 inches high) on the lower hulls and struts. The studs were placed in a vertical column on the inboard and outboard sides of the struts at a point 10% of the strut length aft of the strut leading edge. Studs were also placed around the circumference of the lower hulls at a point 10% of the lower hull length aft of the lower hull nose. Tape with a saw tooth pattern was applied to the rudders at the quater chord for turbulent flow simulation.

EXPERIMENTAL EQUIPMENT AND PROCEDURES

The model was held completely captive with respect to the tow rig and was rigidly attached to a structrual channel through spacer blocks at five points. Two gage assemblies were bolted to the channel, each containing three modular force balances oriented along the body axis to measure longitudinal, lateral, and normal force components. In addition, one modular force balance was mounted on the port side of the bridging structure at the LCG to measure roll force at a prescribed moment arm.

The three gage assemblies were connected to struts mounted on the surface ship towing beam of the Rotating Arm Towing Carriage. Each strut connection had a yaw, pitch, and roll pivot as shown in Figure 3. In addition, each strut could be independently adjusted in the vertical direction to effect changes in draft, trim, and roll angle. This arrangement provided all force components at each of the struts attached to the channel and allowed pitching and yawing moments to be calculated about a reference point half-way between the two struts at the LCG. The moment arm for these calculations was the distance from the reference point (LCG) to the center of the struts.

The roll angle of the model was set by adjusting the height of the strut which was attached to the roll force block gage at the edge of the bridging structure. This strut was adjusted each time the roll angle was set to transmit body axis vertical force only. For each run at a non-zero roll angle the gages were zeroed at standstill, canceling out the roll moment due to buoyancy. Drift angle was set by rotating the surface ship tow beam. The model was set at zero pitch angle throughtout the experiments, except during those runs where pitch effects were studied. Rudder angle was changed by a servo-actuator mounted on the model.

The force measurement outputs were integrated over a standard time of 6 seconds and multiple samples were taken. All forces, angle settings and carriage speed were also stored on stripchart and magnetic digital tape in the carriage borne computer.

Centripetal tares were calculated using the model mass and the carriage rotational speed. Tares were removed and all forces and moments were calculated about the reference point by the computer program described in the next section. Standstill measurements in air on the inertia gear at various roll and trim angles provided the actual CG position of the model which was used in correcting the data.

The design draft was maintained throughout the experimental program at 36.11 centimeters (14.22 inches) model scale. This corresponds to a design displacement of 250 kilgrams (551 pounds). A deep draft condition of 41.2 centimeters (16.22 inches) was also tested. The draft was set by screw jacks and measured optically at the beginning of each condition, then checked periodically throughout the experimental program. The water level was carefully monitored and kept to the proper level.

The experimental program included variations of drift angle, roll angle, speed, draft, rudder deflection angle, propeller RPM, and turn radius. The propeller RPM was adjusted to provide model self-propulsion in the straight ahead condition for each speed and varied to investigate propulsion effects on the data. All the variables were chosen to represent a range of realistic operating conditions and to develop a data base for maneuvering predictions. Combinations of variables were often examined and check points were obtained. The turn

radius was limited by the size of the Rotating Arm Facility and the need to prevent interference and reflection from the wave absorption beach.

ANALYSIS AND PRESENTATION OF DATA

The raw test data, in the form of voltages read from the modular force balances, were filtered and transmitted to the strip chart recorder and the computer. A computer program was utilized to convert the data into nondimensional coefficients and to correct for tares.

The carriage borne Interdata computer program performed the following analysis tasks.

1. Convert the voltages to engineering units.
2. Correct the data for model CG location and centripedal tares.
3. Calculate the resultant hydrodynamic forces and moments about the reference point (full scale CG).
4. Print the raw data, along with the statistical measures of data consistency.
5. Print the resultant forces and moments in English and metric units.
6. Nondimensionalize the results and print out nondimensional quantities.

A sample two page computer print out is shown in Figures 5 and 6. This program and printout allowed immediate examination of the data, about the reference point. Bad data from input errors in carriage speed and angle settings, were readily identified and correction and reanalysis performed without having to repeat a test condition. The computer and operating system on the test facility were very helpful in the efficient conduct of the test.

The data was taken for a matrix of speeds, drift angles, roll angle, rudder angles, and yaw rates. The coupling between all the quantities was determined experimentally so that subsequent simulation would have an empirical basis. The ranges of variables were determined from the expected operating envelope of a ship in a turn including the low speed range for evaluation of the extended-strut rudders operating in the propeller slip stream. This range was also chosen to allow comparison with SWATH-6A data in reference 1.

The nondimensionalized data for yaw moment, side force and roll moment (N', Y', K') were plotted for each speed and draft in the series against yaw rate for a family of drift angles, against rudder angle for a family of yaw rates, and

against roll angle for a family of yaw rates. Nondimensional axial force, X', was also plotted for each speed and draft against rudder angle and drift angle for a family of yaw rates. Representative samples from each series of plots are presented in Figures 7 to 20 in order to illustrate significant trends in the data and for the following discussion of the analysis technique.

The linear derivatives were determined from the aforementioned data plots as the slopes of straight lines through the data. The derivatives both coupled and uncoupled are plotted for each speed and draft in Figures 21 to 40 and are also presented in Table 2.

The nondimensional yaw rate (r') and sway velocity (v') derivatives (denoted by the subscripts r and v respectively) were obtained from plots of nondimensional forces and moment, N', Y' and K' versus r'. An example of the analysis technique can be seen in Figures 7 to 9 which are yaw rate data plots for the 10 knot deep draft test condition with rudder and roll angle fixed at zero degrees. In Figure 7, a line drawn through the zero drift angle data extrapolates to a zero value of N' at zero yaw rate, as it should. The slope represents the nondimensional derivitive N_r'. Similarly, Y_r' and K_r' were determined from figures 8 and 9 respectively. The v' derivatives (N_v', Y_v', K_v') were obtained from curves of force versus drift angle constructed from the zero yaw rate intercepts of the yaw rate plots. The data at zero yaw rate corresponds to the straight line test technique (i.e. infinite radii). However, since the linearity of the data appears to allow reliable extrapolation, the zero yaw rate turning information is provided without actual straight line experiments, therefore saving considerable time and expense.

Yaw rate - sway velocity (v'r') coupled derivatives were also calculated from the yaw rate data plots. In Figures 7 to 9, it can be readily observed that the slopes of the curve of nondimensional forces and moment N', Y', K' versus yaw rate are not constant with varying drift angle. From the changes in slope, the coupled derivatives N_{vr}', Y_{vr}', K_{vr}' were determined. The sway - yaw coupling occured at all but a few test conditions. Figure 10 represents a typical condition where no coupling is evident as is indicated by the constant slope of the data over the range of drift angles.

The nondimensional rudder derivatives $N_{\delta r}'$, $Y_{\delta r}'$ and $K_{\delta r}'$ were determined from plots of nondimensional forces and moment N', Y', and K' versus rudder angle (δ_r). Rudder angles from -30 to +20 degrees were investigated. The data were linear throughout the range of rudder angles for all but a few test conditions, at the 25 and 30 knot speeds where the rudder induced forces and moments dropped off slightly at the largest rudder deflections. The effect of drift angle on yaw moment, side force and roll moment due to the rudder was negligible for all speeds and yaw rates; that is, the slope of the data points remained constant for various drift angles. This lack of coupling is clearly illustrated in Figure 11 which is the plot of nondimensional yaw moment, N', versus rudder angle δr for the 20 knot, design draft test condition at a nondimensional yaw rate of 0.103.

The effect of yaw rate on yaw moment, side force and roll moment due to rudder was also negligible over the range of speeds tested, as illustrated in Figure 12. Figure 12 is the plot of side force versus rudder angle at the 15 knot deep draft test condition, and the constant slope over a range of yaw rates clearly indicates the lack of coupling. This behavior was typical for nondimensional yaw moment and nondimensional roll moment data as well.

The nondimensional roll derivatives N_{ϕ}', Y_{ϕ}', and K_{ϕ}', were determined from plots of nondimensional forces and moment N', Y' and K' versus roll angle (ϕ). Roll angles through $\pm$ 4 degrees were investigated. The effects of roll angle on the forces and moments were relatively small as might be expected by the wall sided nature of the SWATH design. Coupling between quantities was investigated and it was found that drift-roll coupling and rudder-roll coupling were negligable, while slight coupling between yaw rate and roll angle was observed at some conditions. Figures 13 to 18 are representative samples of the data plots used for determining coupling. Figure 13 is typical of the data in that the constant slope of the data over the range of drift angles indicates no drift/roll coupling. Figure 14 presents the typical trend of the effect of rudder angle on roll derivatives and again the constant slope of the data indicates no coupling.

The coupling between yaw rate and roll angle occurred only at certain conditions and was small in magnitude. Figure 15 presents the plot of nondimen-

sional yaw moment vs roll angle at the 10 knot deep draft condition for two yaw rates. It is an example of where there is no coupling and in fact, no effect on yaw moment due to roll angle (i.e. both $N_\phi = 0$, and $N_{r\phi} = 0$). As the speed was increased to 20 and then 25 knots (Figures 16, and 17), slight changes in slope occurred. In Figure 16, the slope of the data at a radius of .208 increased slightly while at 25 knots, Figure 17, the slope at both radii increased. Figure 18 is the plot of side force versus roll angle for the 20 knot deep draft condition and again the change in slope indicates slight yaw rate/roll angle coupling.

A sample plot of axial force (X') versus rudder angle for the 15 knot deep draft condition is presented in Figure 19. The model was propelled at the self propulsion point so the axial force (less frictional allowance) is close to zero at zero rudder angle. At large rudder angles there is an increase in drag that is very apparent as a negative axial force. The effect is approximately quadratic with rudder angle, and therefore yields the $X_{\delta\delta}'$ derivative.

An example of the effect of drift angle on axial force is given in Figure 20 for three radii. The axial force is approximately quadratic, yielding the X_{vv}' derivative.

DISCUSSION OF RESULTS

As shown in the previous section, the linearity of the data permitted calculation of the hydrodynamic derivatives, both coupled and uncoupled, from slope and changes in slope of the force and moment data. These derivatives correspond to the standard Taylor series horizontal plane hydrodynamic maneuvering coefficients described in reference 2. While the final evaluation of the SWATH-6E maneuvering performance must await simulation results, some pertinent observations can be made.

In general, the magnitudes and signs of the derivatives are as expected for SWATH ships. Also, the magnitude of the nondimensional derivatives generally increase with increasing draft.

By comparison, the SWATH-6E derivatives appear to be much less speed dependent than those of the shorter strut SWATH-6A. The SWATH-6A derivatives are

found in reference 1. The SWATH-6E exhibits strong yaw rate-sway velocity (vr) coupling, not seen on previous SWATH-6 series tests. The magnitude of this coupling is significant as seen in Figures 33 thru 35 and an increase in magnitude with draft is evident.

Coupling is also observed between yaw rate and roll angle. As seen in Figures 36, 37, and 38 this coupling occurs only at certain conditions and is generally of smaller magnitude than vr coupling.

The effectiveness of the SWATH-6E rudders is much improved over the 6A spade rudders. The rudder effectiveness derivatives, shown in Figures 27 thru 29 are generally much less speed dependent than the 6A rudders and are also of greater magnitude. This is due in part to the lack of free surface effects since the 6E rudders were fully submerged. The rudder effectiveness also improves with increased draft, particularly at the higher speeds. At 25 and 30 knots a decrease in the magnitude of the derivatives at design draft is observed. This may be due to the observed rudder ventilation at design draft. This problem is model scale dependent and could be avoided in a full scale ship design.

In order to get an idea of the relative turning performance of the SWATH-6E; an estimate of the steady state turn diameter, dynamic stability criterion, and the steady state drift angle may be made based on linear theory.

The stability criterion, C, is given in reference 2 as:

$$C = Y_v'(N_r' - m'x_g') - N_v'(Y_r' - m') > 0 \qquad [1]$$

The equation for steady state turn radius per ship length is given in reference 2 as:

$$R/L = -\frac{1}{\delta r}\,\frac{C}{Y_v'N_{\delta r} - N_v'Y_{\delta r}} \qquad [2]$$

Steady state drift angle, β, is given by:

$$\beta = \delta_r \left[\frac{N_{\delta r}(Y_r'-m') - Y_v'(N_r'-m'x_g')}{Y_v'(N_r'-m'x_g') - N_v'(Y_r'-m')}\right] \qquad [3]$$

The dynamic stability criterion for the SWATH-6AS (6A with spade rudder) and 6E are compared in Table 3. The larger values of C for the 6E indicate that it is more directionally stable than the 6A for both drafts and at every speed. The steady turn radiusper unit ship length and steady drift angle for the 6A and 6E are presented in Table 4. The SWATH 6E exhibits a smaller turn radius at nearly every speed, with a maximum turn diameter of 6 ship lengths. At 10 and 15 knots deep draft, the 6A has a smaller turn radius than the 6E. This is probably because the 6A spade rudders have more projected area at deep draft.

The lack of speed dependence of the 6E derivatives is clearly seen in the lack of variation of R/L over the rango of speeds, and particularly in comparison to the 6A.

The extended strut design was originally intended to improve low speed maneuvering, however, these preliminary results indicate that the 6E is a better configuration throughout the speed range.

CONCLUSIONS

The extended strut SWATH-6E exhibited strong yaw rate-sway velocity and yaw rate-roll angle coupled nondimensional derivatives, not previously observed in shorter strut SWATH-6 series experiments.

The maneuvering performance of the SWATH-6E does not vary greatly with forward speed.

The SWATH-6E is directionally stable, and is more stable than previous SWATH-6 series configurations, as expected for an extended strut design.

The SWATH-6E rudders exhibit much improved rudder effectiveness over the SWATH-6A spade rudder design.

In general, the SWATH-6E configuration provides excellent stability and maneuvering performance, particularly at high speeds.

REFERENCES

1. Fein, J.A., and Waters, R.T., "Rotating Arm Experiments for SWATH-6A Maneuvering Prediction." DTNSRDC/SPD-698-01 July 1976.

2. Comstock, J.P., Ed., "Principles of Naval Architecture." SNAME 1967.

TABLE 1 - GEOMETRIC AND PHYSICAL CHARACTERISTICS OF THE SWATH 6E

Length, Overall feet (meters)	11.74	(3.58)
Length, Strut feet (meters)	11.18	(3.41)
Length, Lower Hull feet (meters)	10.67	(3.25)
Strut Setback feet (meters)	0.57	(0.17)
Beam, Maximum feet (meters)	4.00	(1.22)
Beam, Strut Centerline feet (meters)	3.33	(1.02)
Draft, Maximum feet (meters)	1.18	(0.36)
Draft, Strut feet (meters)	0.52	(0.16)
Hull Diameters, Maximum feet (meters)	0.67	(0.20)
Strut width, Maximum feet (meters)	0.24	(0.07)
Displacement, Design Draft LTSW (Metric Tonnes)	0.255	(0.259)
Displacement, Deep Draft LTSW (Metric Tonnes)	0.265	(0.269)
Distance, Nose to Center of Gravity feet (meters)	5.32	(1.62)
Distance, Nose to Rudder Hinge Axis feet (meters)	11.31	(3.45)
Rudders: Chord feet (meters)	0.58	(0.18)
Span feet (meters)	0.80	(0.24)
Aspect Ratio	1.37	
Lateral Area feet^2 (Meters^2)	0.463	(0.14)
Thickness/Chord Ratio	.21	(NACA 0021 Section)

TABLE 2

SWATH 6E NONDIMENSIONAL DERIVATIVES - DESIGN DRAFT

Derivative	Speed (knots)					
	7	10	15	20	25	30
N_r'	-0.0098	-0.0117	-0.0113	-0.0123	-0.0163	-0.0167
Y_r'	0.0283	+0.0277	0.0230	0.0243	0.0303	0.0220
K_r'	-0.0049	-0.0051	-0.0046	-0.0053	-0.0060	-0.0045
N_v'	-0.0201	-0.0251	-0.0280	-0.0165	-0.0345	-0.0295
Y_v'	-0.0560	-0.0560	-0.0604	-0.0762	-0.0438	-0.0525
K_v'	0.0125	0.0118	0.0101	0.0147	0.0077	0.0088
$N_{\delta r}'$	-0.0095	-0.0099	-0.0090	-0.0090	-0.0091	-0.0074
$Y_{\delta r}'$	0.0188	0.0202	0.0181	0.0180	0.0177	0.0155
$K_{\delta r}'$	-0.0034	-0.0038	-0.0036	-0.0034	-0.0035	-0.0030
N_ϕ'	0.00036	0	0.00322	0.00036	0.00573	0.00358
Y_ϕ'	0.00716	0.00215	-0.00430	0	-0.00788	0.00859
K_ϕ'	0.00036	0	0.00136	0.00036	0.00025	-0.00222
Coupled Derivatives						
N_{vr}'	0.0481	0.0201	0.0251	0.0158	0.0158	0
Y_{vr}'	-0.084	-0.1140	-0.1290	-0.0880	-0.1160	-0.2190
K_{vr}'	0	0.0172	0.0301	0	0.0187	0.0301
$N_{r\phi}'$	0	0	0	0.08126	0	0
$Y_{r\phi}'$	0	0	-0.09534	-0.13625	0	0
$K_{r\phi}'$	0.00409	0.01427	0.01637	0.02379	0	0
$X_{\delta r\delta r}'$	0.01888	0.01970	0.01723	0.01970	0.02585	0.02052
X_{vv}'	-0.01353	-0.01910	-0.01139	-0.00955	-0.0185	-0.00887

TABLE 3

SWATH 6E - NONDIMENSIONAL COEFFICIENTS - DEEP DRAFT

Derivatives	7	10	15	20	25	30
N_r'	-0.0137	-0.0143	-0.0147	-0.0152	-0.0220	-0.0223
Y_r'	0.0370	0.0317	0.0303	0.0303	0.0303	0.0253
K_r'	-0.0056	-0.0052	-0.0065	-0.0060	-0.0067	-0.0049
N_v'	-0.0280	-0.0374	-0.0345	-0.0287	-0.0575	-0.0445
Y_v'	-0.0762	-0.0747	-0.0740	-0.0862	-0.0690	-0.0453
K_v'	0.0103	0.0111	0.0126	0.0144	0.0109	0.0071
$N_{\delta r}'$	-0.0095	-0.0099	-0.0090	-0.0095	-0.0105	-0.0092
$Y_{\delta r}'$	0.0204	0.0208	0.0192	0.0193	0.0212	0.0179
$K_{\delta r}'$	-0.0039	-0.0038	-0.0036	-0.0036	-0.0040	-0.0035
N_ϕ'	0	0	0.00573	0.00430	0.00967	0.00501
Y_ϕ'	-0.00286	0	-0.00859	0	-0.00609	-0.00286
K_ϕ'	0	0.00072	0.00201	0.00057	0.00115	-0.00054
Coupled Derivatives						
N_{vr}'	0.0402	0.0402	0.0467	0.0417	0.0467	0
Y_{vr}'	-0.1904	-0.2536	-0.2026	-0.1631	-0.0960	-0.2457
K_{vr}'	0.0244	0.0373	0.0014	0.0459	0.0057	0.00602
$N_{r\phi}'$	0	0	0	0.03406	0	0
$Y_{r\phi}'$	0	0	-0.04434	-0.14310	-0.04767	0
$K_{r\phi}'$	0.02797	0	0	0.01028	-0.02188	-0.00913
$X_{\delta r\delta r}'$	0.02216	0.02380	0.02216	0.02462	0.03119	0.02708
X_{vv}'	-0.00778	-0.01706	-0.01148	-0.02371	-0.02029	-0.02194

TABLE 4

COMPARISON OF THE DYNAMIC STABILITY CRITERION, C*, FOR SWATH 6E AND SWATH 6AS AT DESIGN AND DEEP DRAFT CONDITIONS

	SWATH 6E		SWATH 6AS	
SPEED, KTS	DESIGN	DEEP	DESIGN	DEEP
7	.00170	.00325	--	--
10	.00187	.00321	.00140	.00210
15	.00223	.00312	.00153	.00220
20	.00232	.00329	.00144	.00297
25	.00246	.00446	.00186	.00303
28	--	--	.00133	--
30	.00210	.00284	--	--

* Nondimensionalization in these calculations based on lower hull length.

TABLE 5

STEADY STATE TURN RADIUS PER SHIP LENGTH*
AND STEADY STATE DRIFT ANGLE, β, FOR THE SWATH 6E AND SWATH 6A
WITH A 27 DEGREE RUDDER ANGLE

DESIGN DRAFT

Speed, Knots	SWATH 6E R/L*	β, deg.	SWATH 6A - SPADE RUDDERS R/L*	β, deg.
7	2.09	0.60	--	--
10	2.15	1.78	1.93	1.47
15	2.06	2.56	2.23	2.10
20	2.50	2.37	3.20	1.59
25	2.90	2.21	6.10	0.94
28	--	--	4.57	1.29
30	3.02	3.99	--	--

DEEP DRAFT

7	2.88	0.56	--	--
10	2.56	1.43	1.53	2.14
15	2.78	1.74	2.10	1.94
20	2.86	1.66	3.72	0.57
25	2.84	2.78	4.61	1.27
30	2.85	4.50	--	--

* Length, L, used in above nondimensionalization corresponsds to LOA.

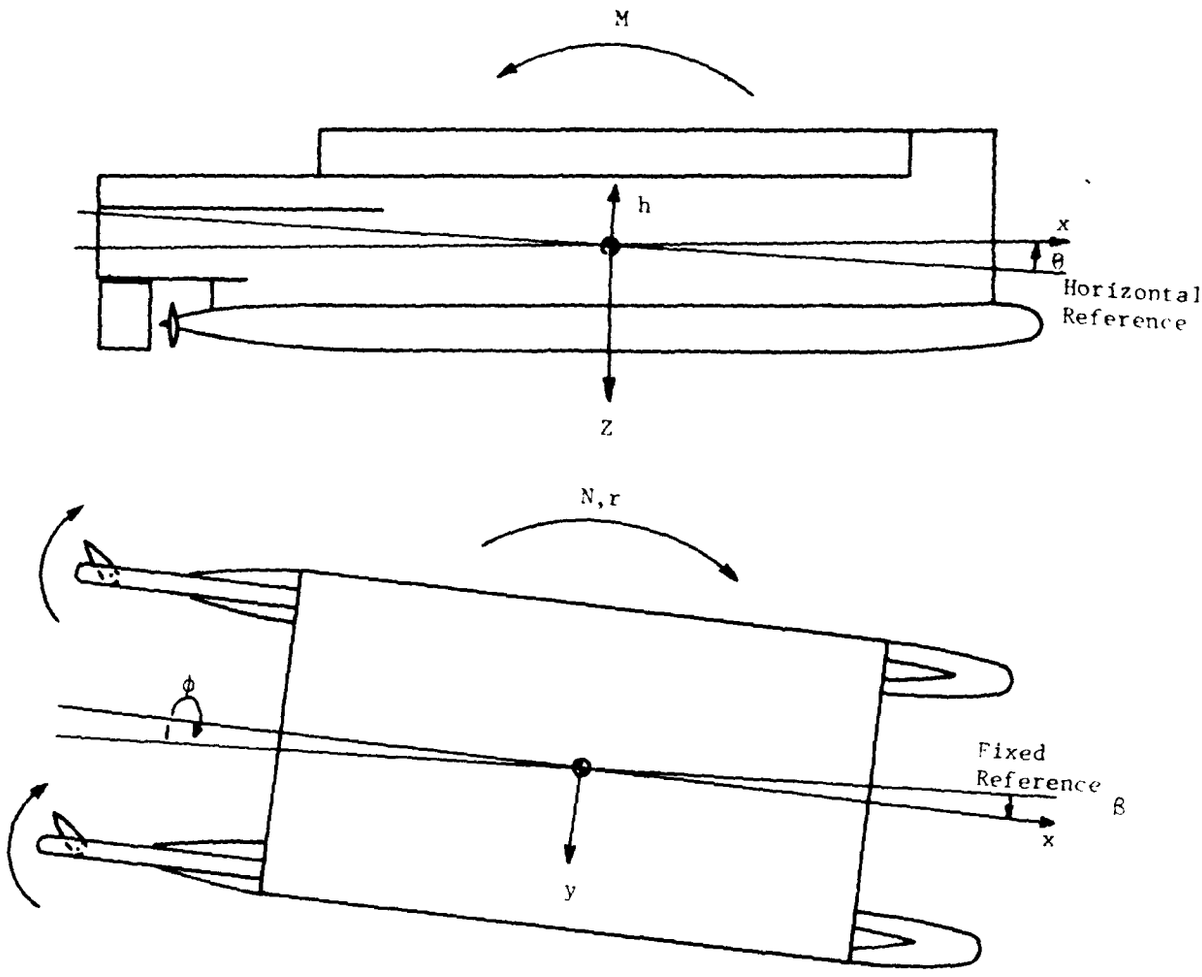

Figure 1 - Schematic Indicating Coordinate Systems and Positive Directions of Measured Values

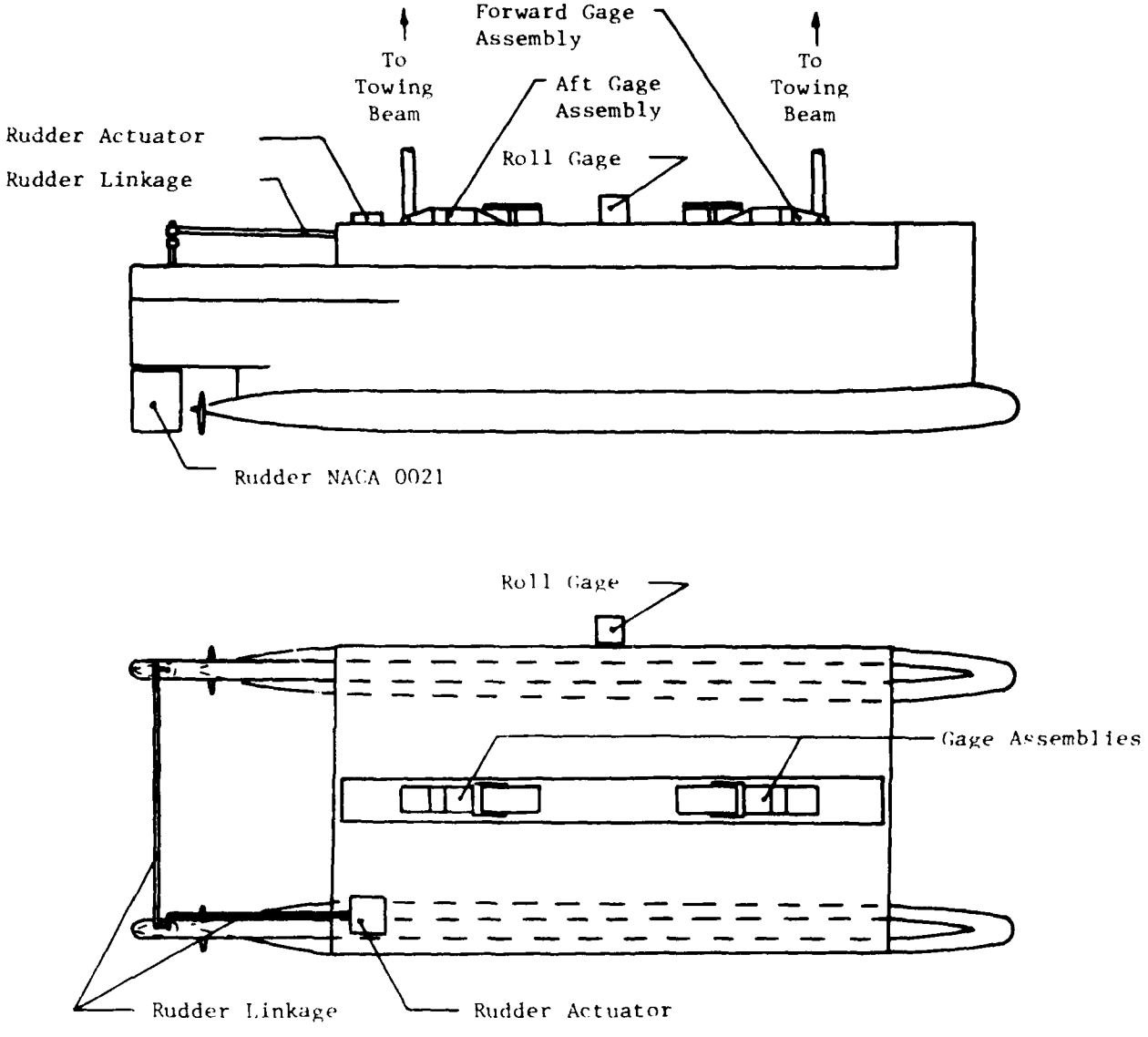

Figure 2 - Schematic for the SWATH-6E Model Showing Location of the Rudder and Gage Assemblies

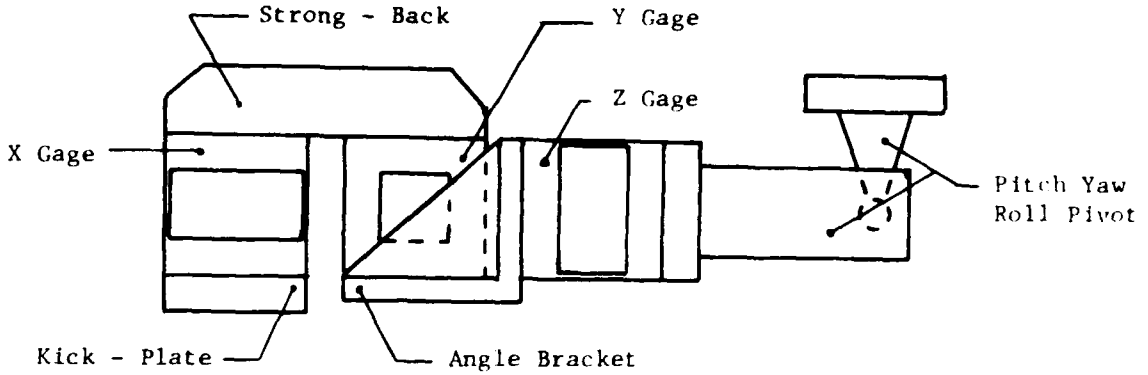

FOREWARD GAGE
ASSEMBLY

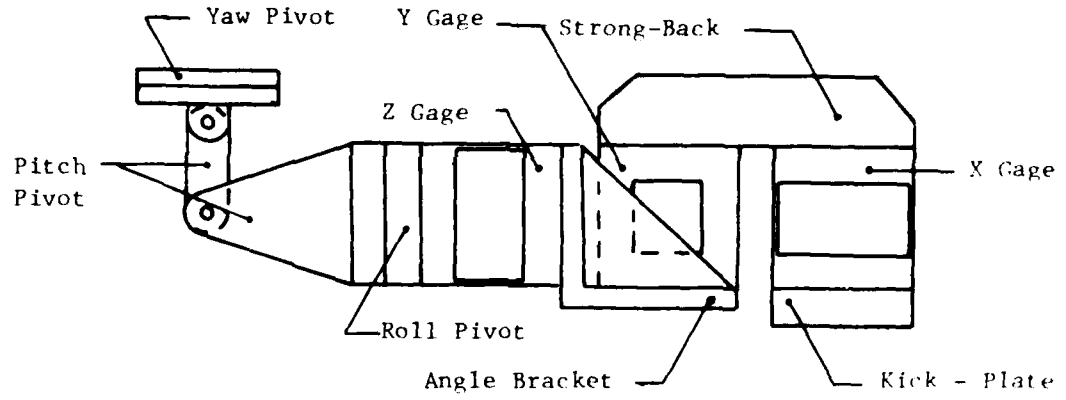

AFT GAGE
ASSEMBLY

Figure 3 - Schematic of the Foreword and Aft Block Gage Assemblies use on the SWATH-6E

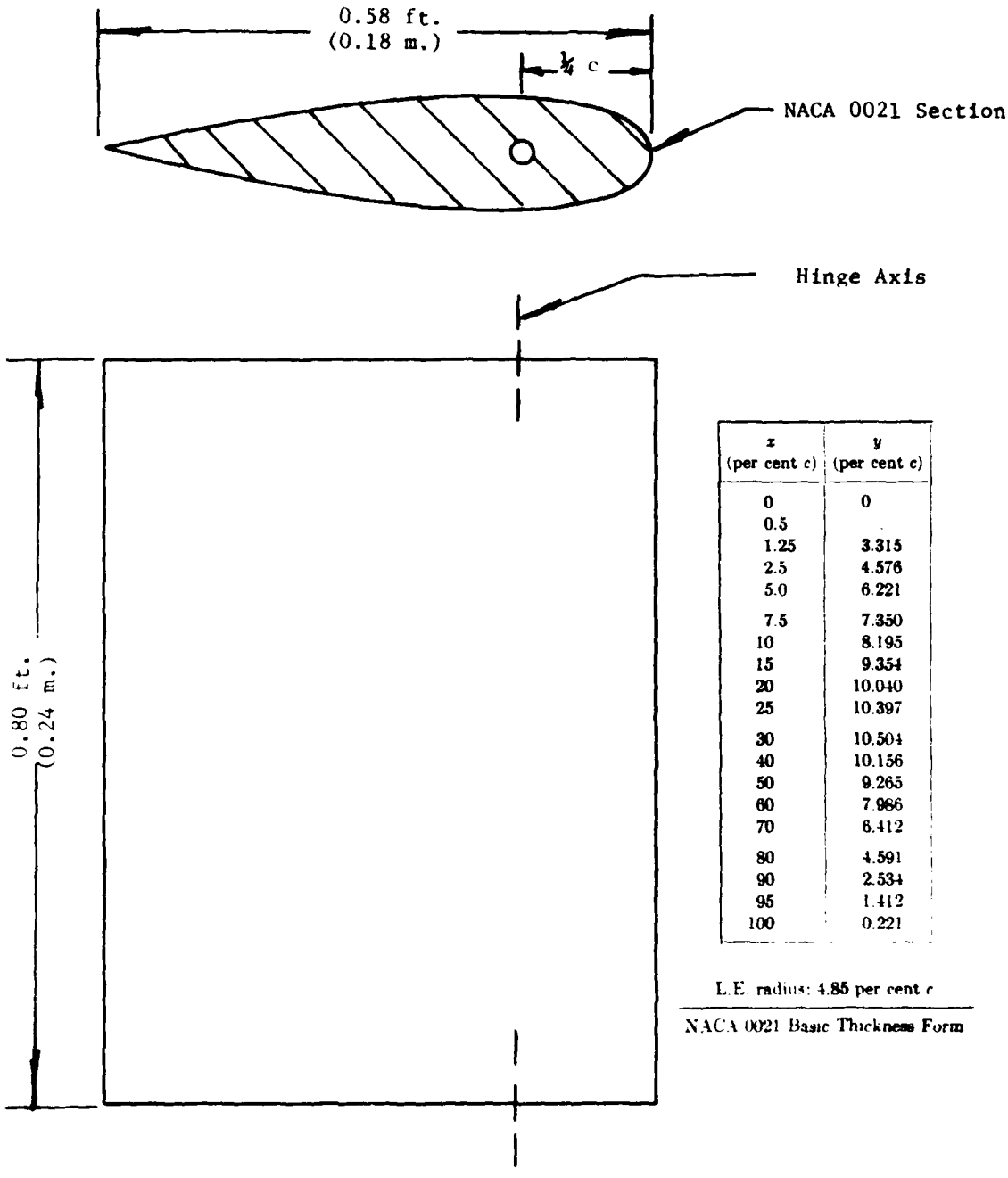

x (per cent c)	y (per cent c)
0	0
0.5	
1.25	3.315
2.5	4.576
5.0	6.221
7.5	7.350
10	8.195
15	9.354
20	10.040
25	10.397
30	10.504
40	10.156
50	9.265
60	7.966
70	6.412
80	4.591
90	2.534
95	1.412
100	0.221

L.E. radius: 4.85 per cent c

NACA 0021 Basic Thickness Form

Figure 4 - SWATH-6E Rudder Profile

ROTATING ARM SWATH 6E - TURNING PERFORMANCE TEST 3 AUG/SEPT 82

PITCH ANGLE (DEG) : 0.0000
ROLL ANGLE (DEG) : 0.0000
IEEP DRAFT

TURNING RADIUS : 38.10 FT

MEAS SPEED = 2.11 KNOTS
NOMN SPEED = 2.11 KNOTS

RUNS : 1010.: 0.000 - 6.400

TOTAL TIME : 6.400 SEC

	CHAN			CALIB	GAIN	MEAN	STDDEV	ROOTSQ
1	X FWD	LBS		-2.000E+01	1.000E+00	1.866E+00	1.075E+00	1.521E+00
2	[illegible]	LBS		+2.000E+01	1.000E+00	-1.295E-01	5.726E-02	8.101E-02
3	[illegible]	LBS		[illegible]	1.000E+00	-1.826E+01	7.538E-01	1.066E+00
4	[illegible]	LBS		-4.000E+01	1.000E+00	2.074E+01	7.815E-01	1.105E+00
5	[illegible]	LBS		[illegible]	.000E+00	3.345E+00	5.422E-01	7.682E-01
6	[illegible]	LBS		[illegible]	1.000E+00	1.674E+00	4.035E-01	5.555E-01
7	[illegible]	LBS		[illegible]	1.000E+00	5.445E+00	8.605E-01	1.217E+00
8	[illegible]	LBS		[illegible]	1.000E+00	4.013E+00	5.524E-03	7.812E-03
9	[illegible]	LBS		[illegible]	1.000E+00	7.360E+00	1.001E-01	1.416E-01
10	[illegible]	LBS		[illegible]	1.000E+00	1.333E+00	1.867E+00	2.640E+00
[illegible]	[illegible]	[illegible]		[illegible]	1.000E+00	-2.303E-01	4.072E-03	5.759E-03

Figure 5 - First Page of Computer Printout Showing List of Data for Each Channel

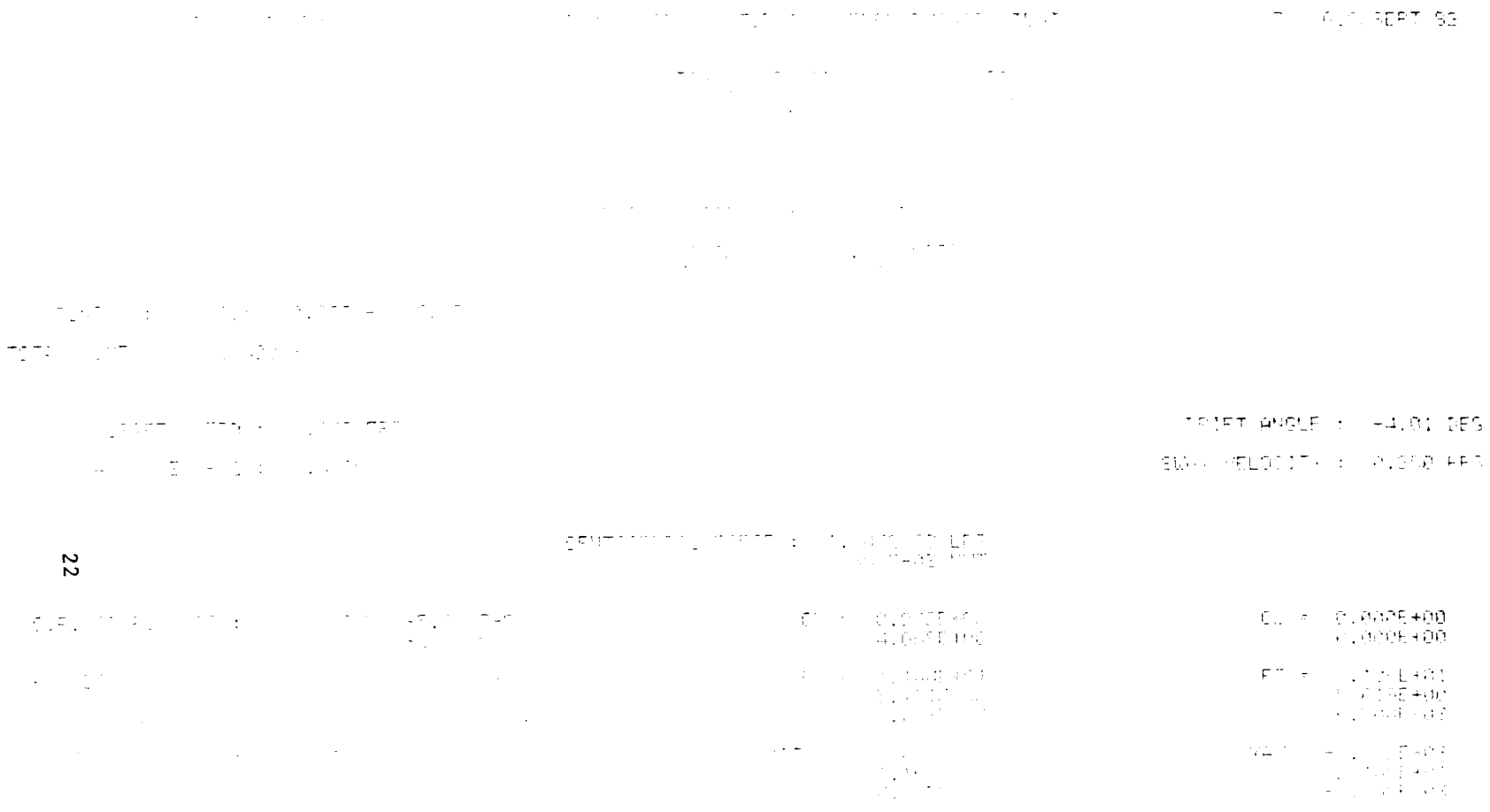

Figure 6 - Second Page of Computer Printout Showing List of Forces and Moments About Reference Point

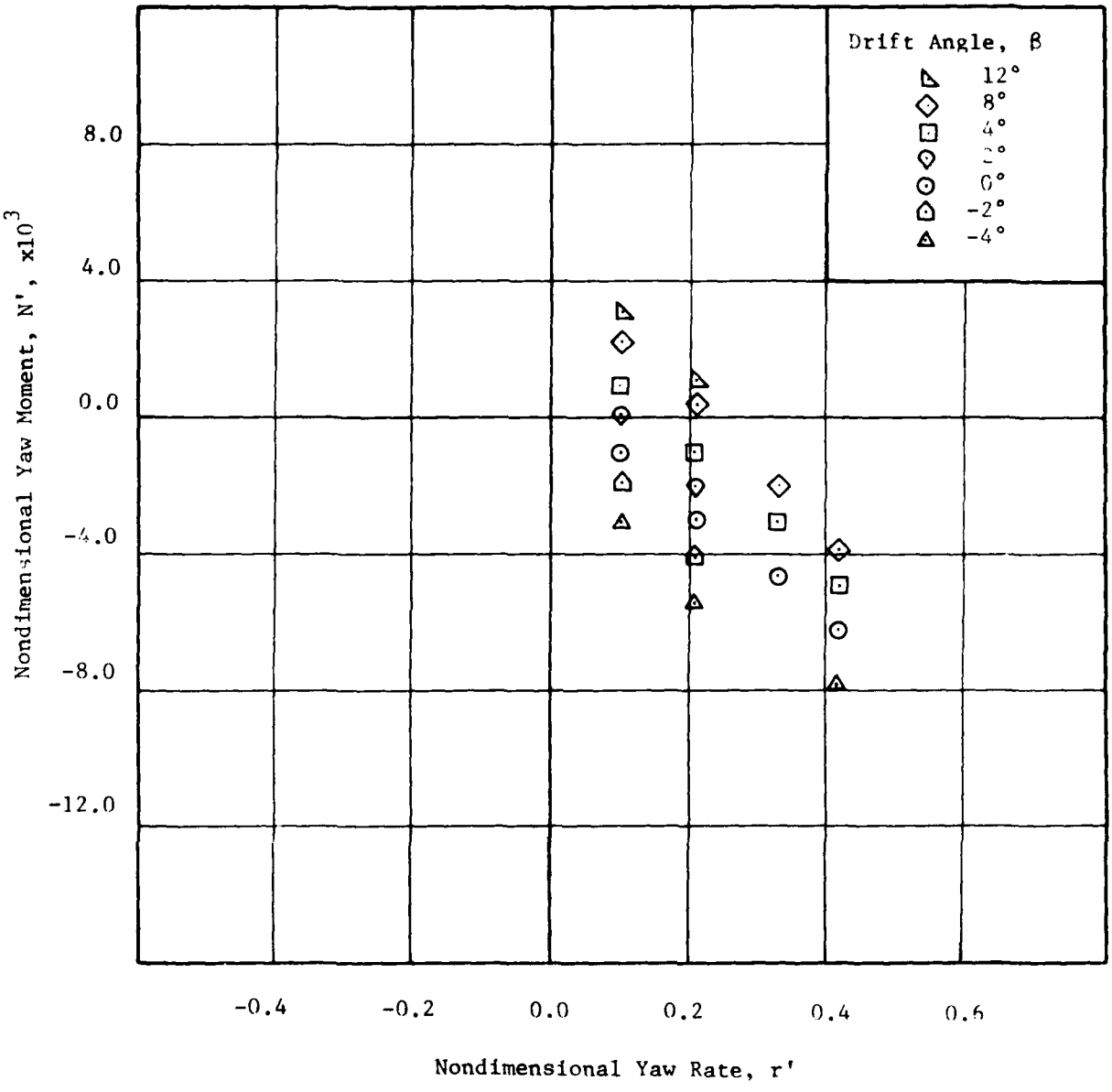

Figure 7 - Variation of Nondimensional Yaw Moment with Nondimensional Yaw Rate for a Series of Drift Angles at a Full Scale Speed of 10 knots at Deep Draft

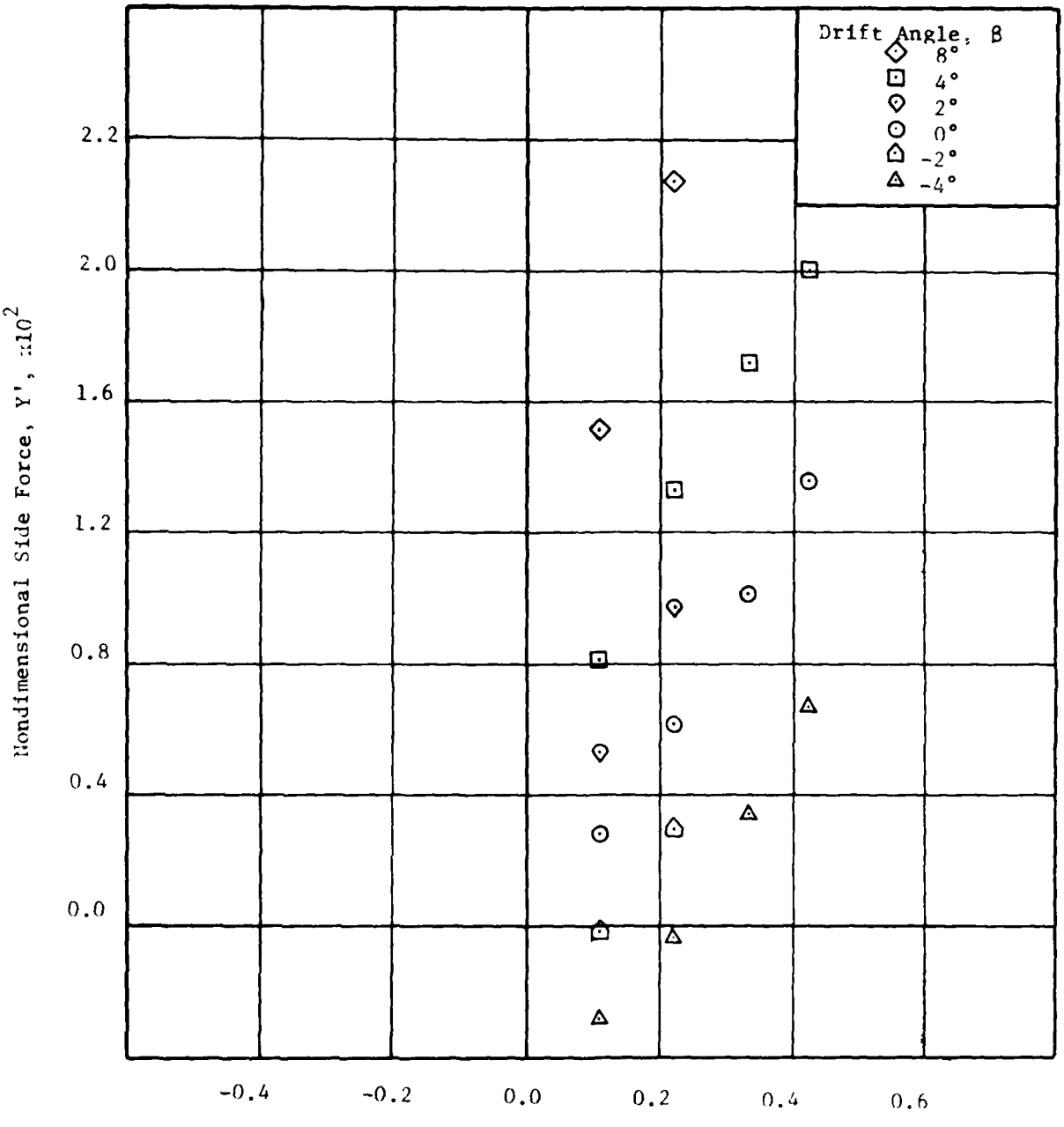

Figure 8 - Variation of Nondimensional Side Force with Nondimensional Yaw Rate for a Series of Drift Angles at a Full Scale Speed of 10 Knots at Deep Drift

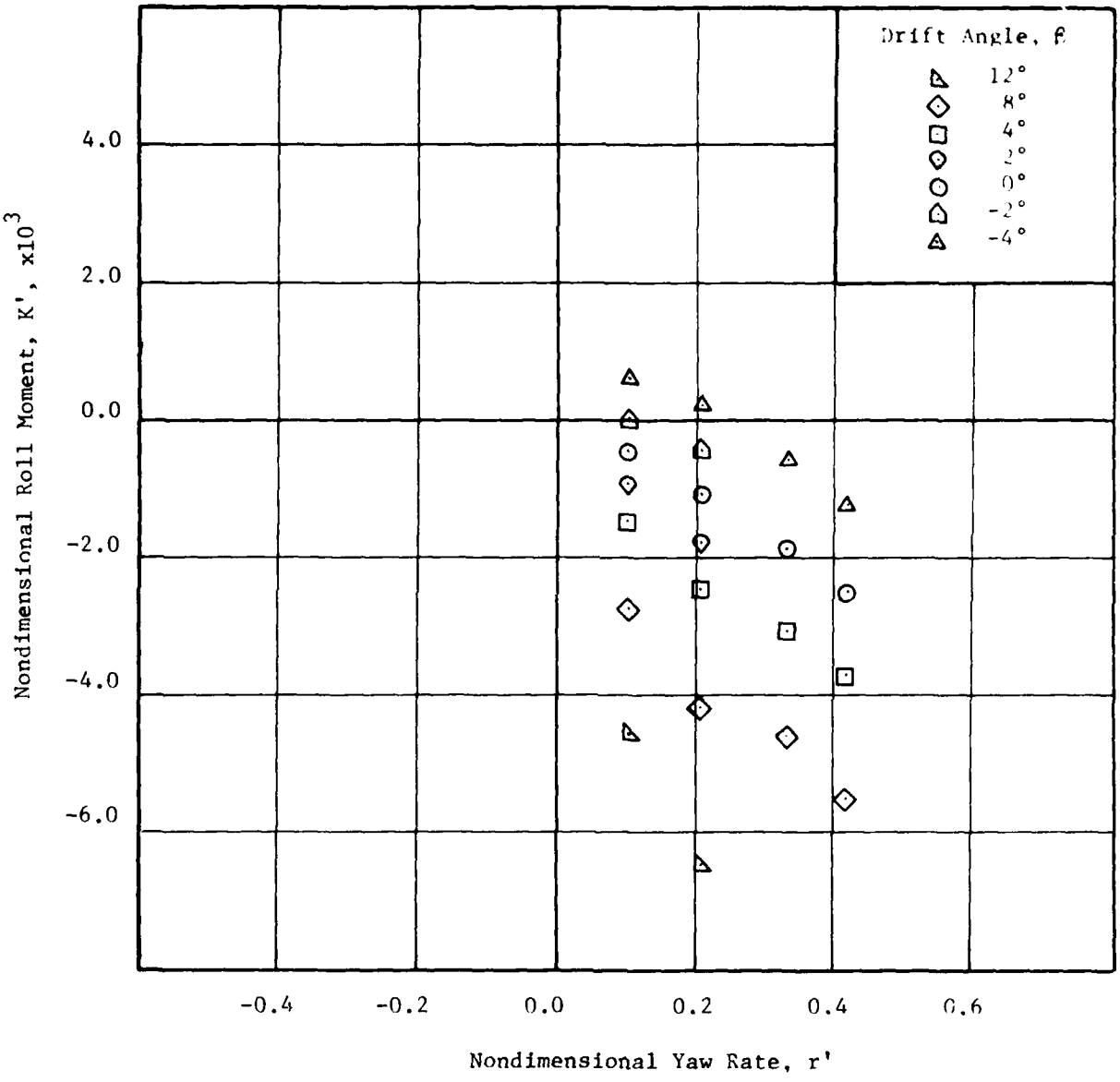

Figure 9 - Variation of Nondimensional Roll Moment with Nondimensional Yaw Rate for a Series of Drift Angles at a Full Scale Speed of 10 Knots at Deep Draft

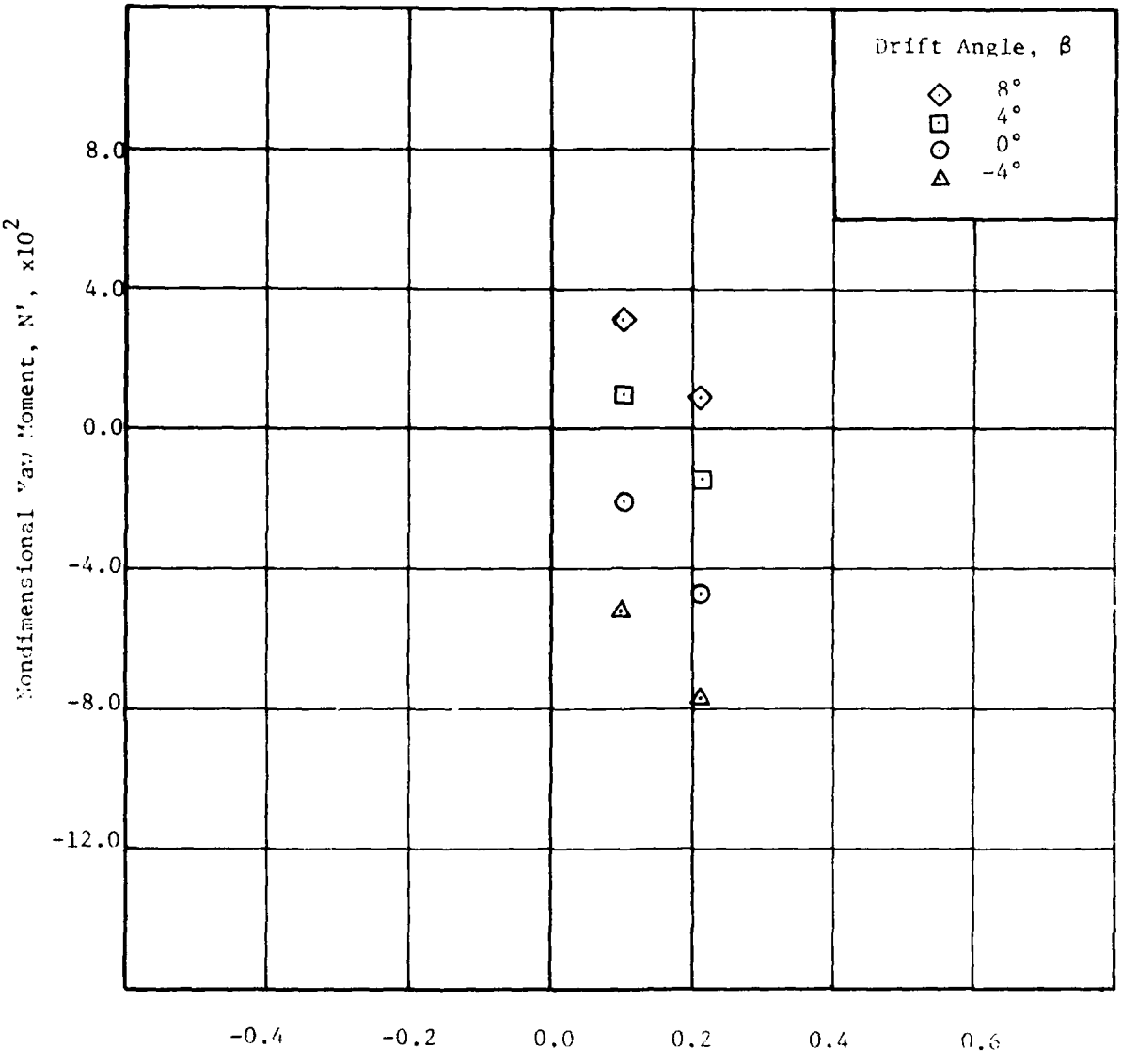

Figure10 - Variation of Nondimensional Yaw Moment with Nondimensional Yaw Rate for a Series of Drift Angles at a Full Scale Speed of 30 Knots at Deep Draft

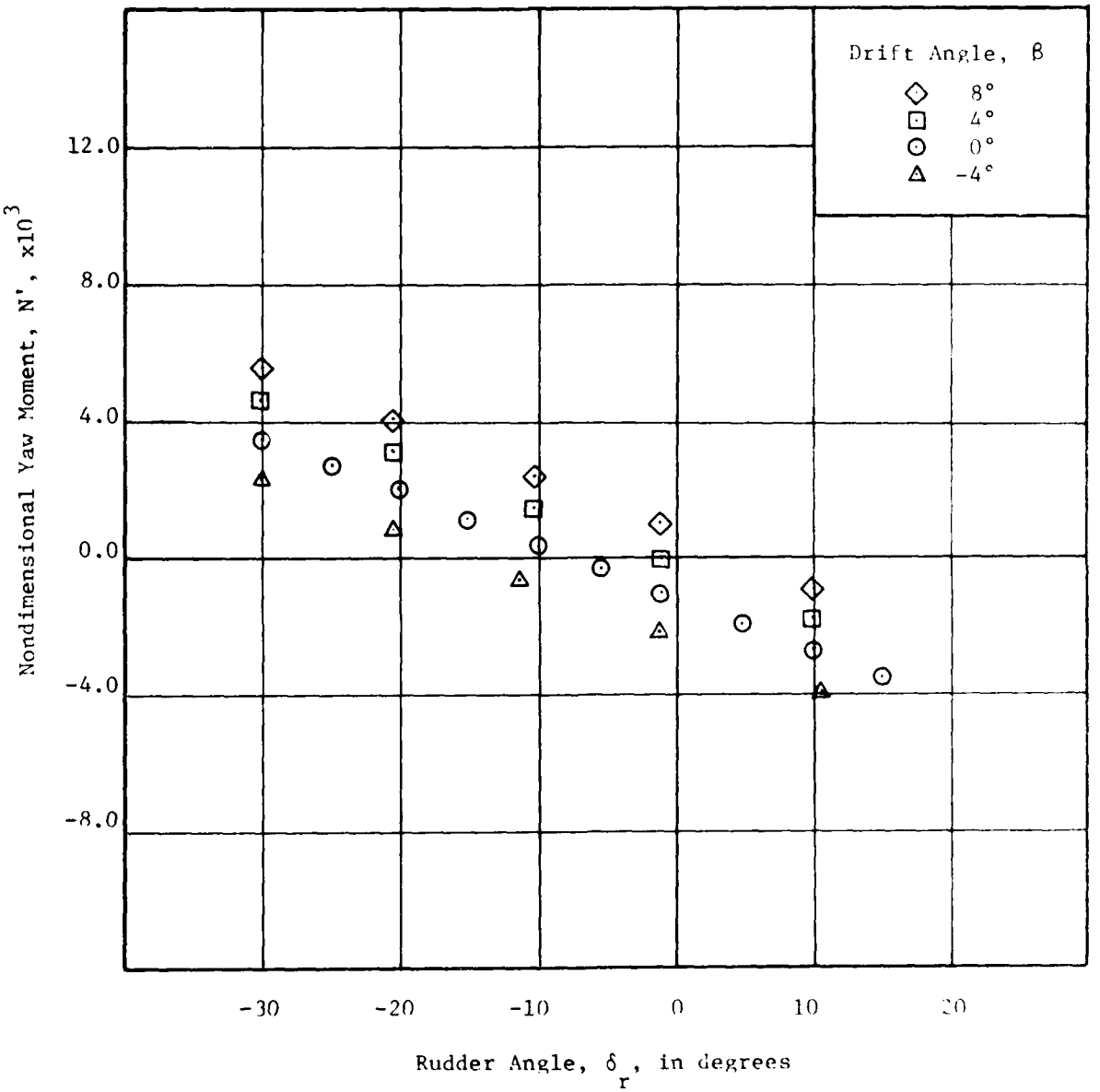

Figure 11- Variation of Nondimensional Yaw Moment with Rudder Angle for a series of Drift Angles at a Full Scale Speed of 20 Knots and a Nondimensional Yaw Rate of 0.103 at Design Draft

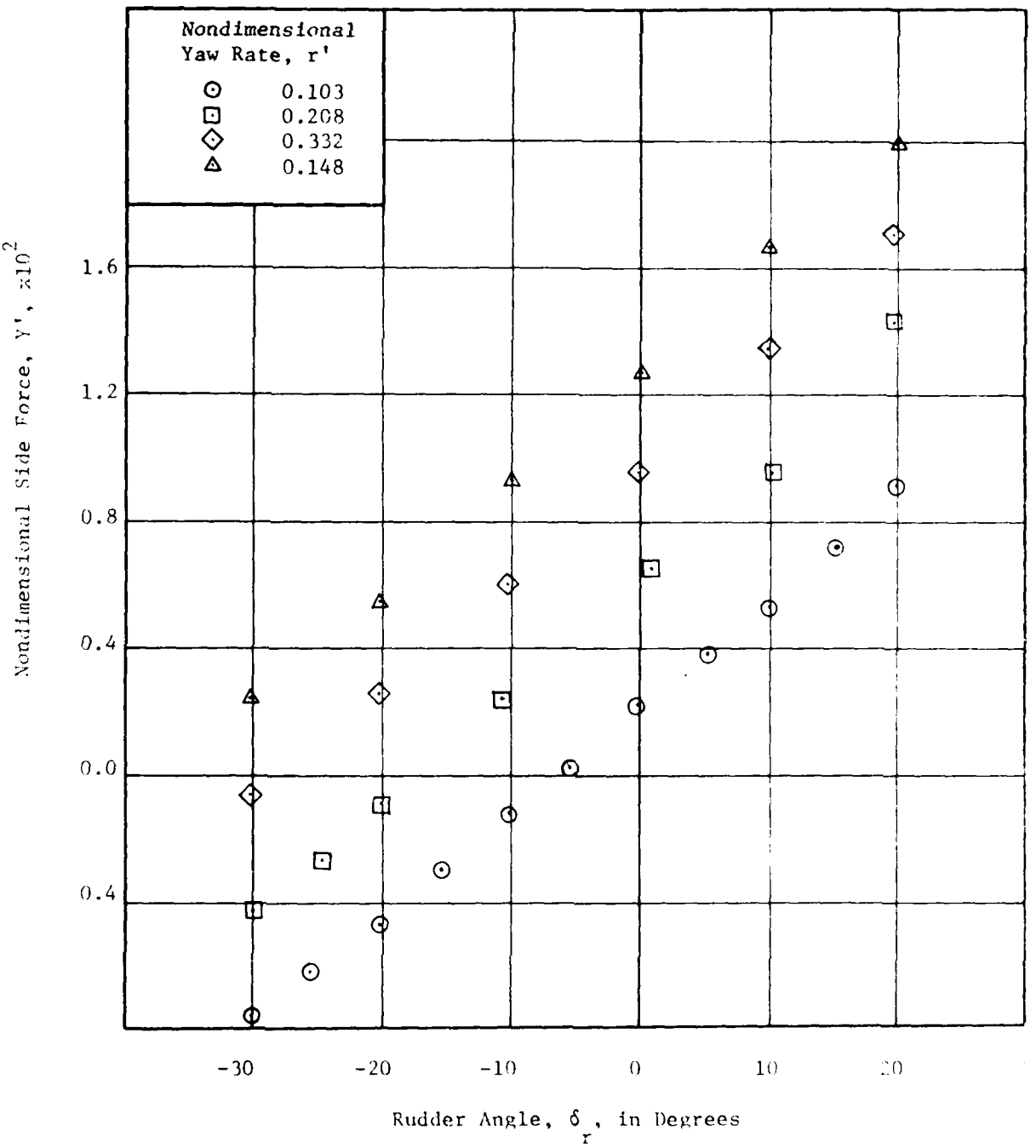

Figure 12- Variation of Nondimensional Side Force with Rudder Angle for a Series of Nondimensional Yaw Rate at a Full Scale Speed of 15 knots at Deep Draft

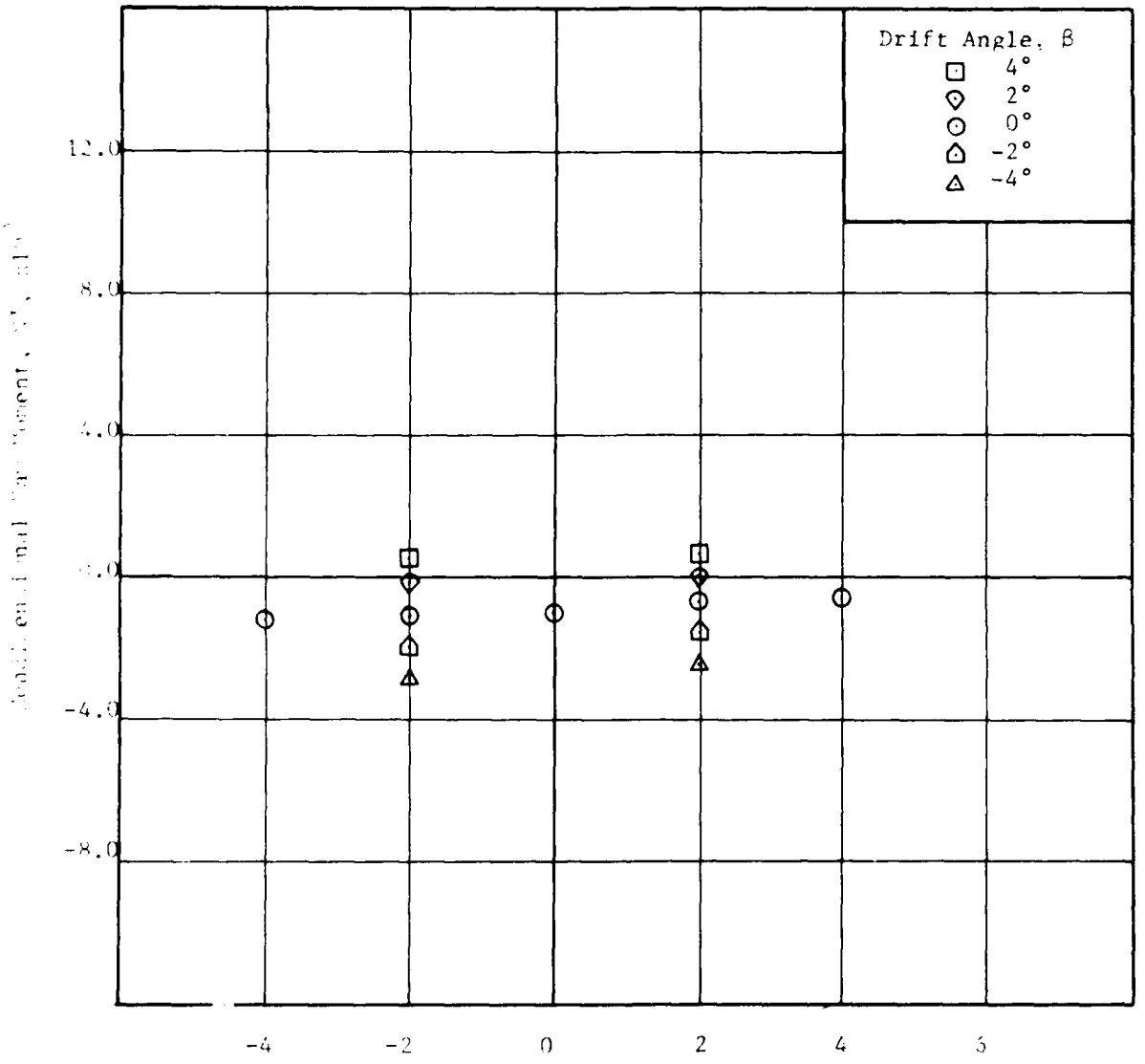

Figure 13- Variation of Nondimensional Yaw Moment with Roll Angle for a Series of Drift Angles at a Full Scale Speed of 15 Knots and a Nondimensional Yaw Rate of 0.103 at Design Draft

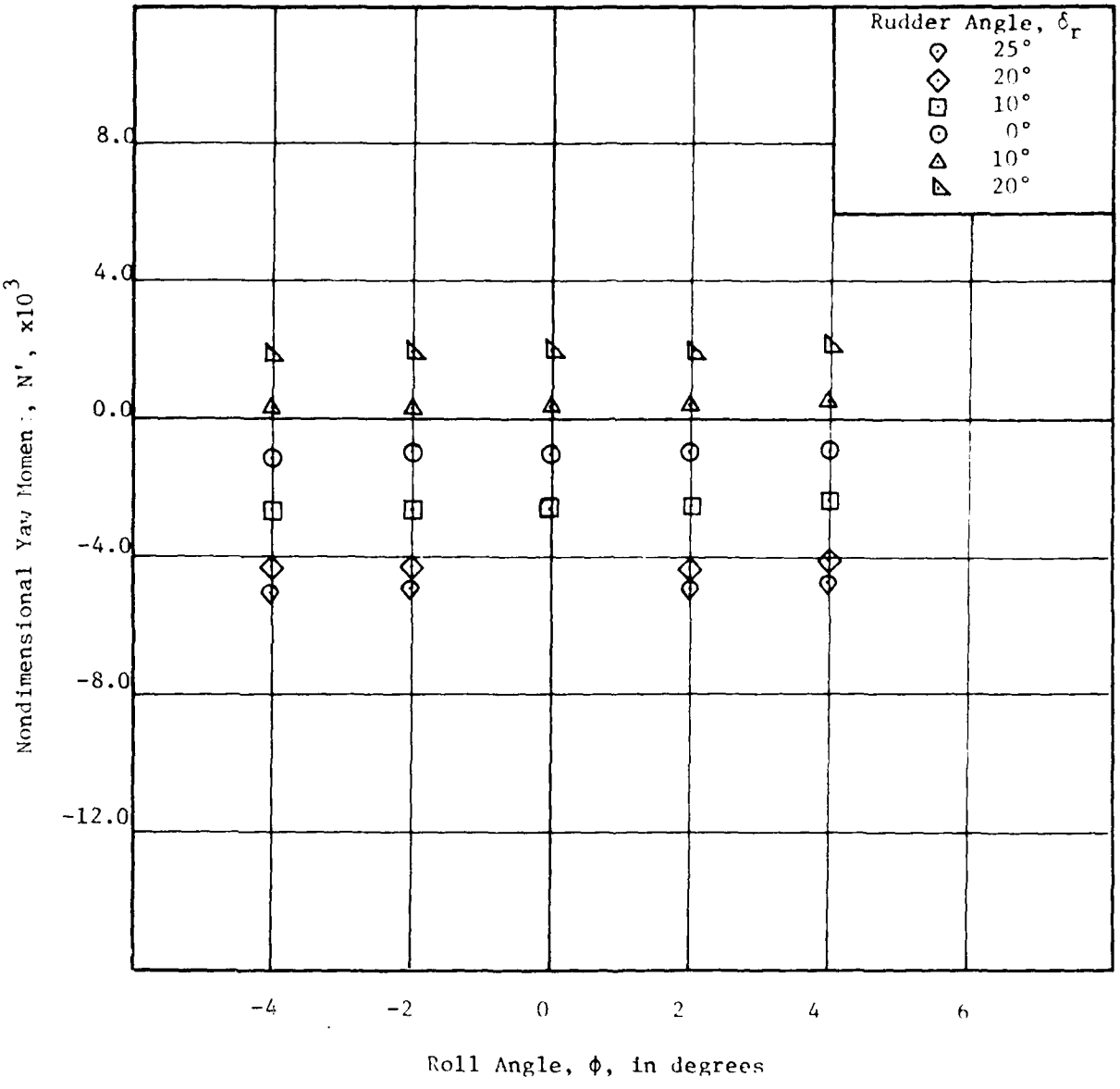

Figure 14- Variation of Nondimensional Yaw Moment with Roll Angle for a Series of Rudder Angles at a Full Scale Speed of 20 Knots and a Nondimensional Yaw Rate of 0.103 at Design Draft

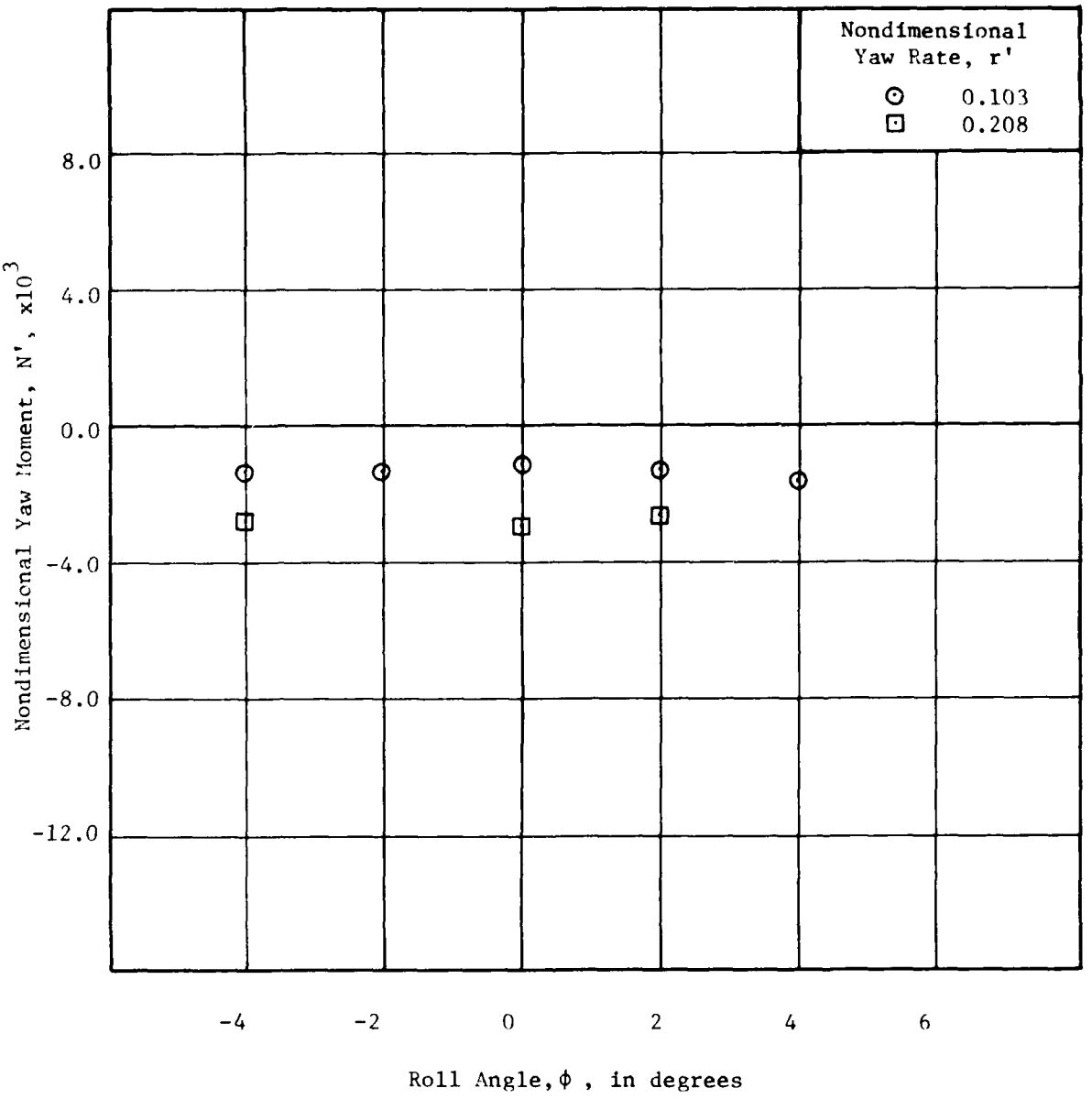

Figure 15 - Variation of Nondimensional Yaw Moment with Roll Angle for Two Nondimensional Yaw Rates at a Full Scale Speed of 10 Knots at Deep Draft

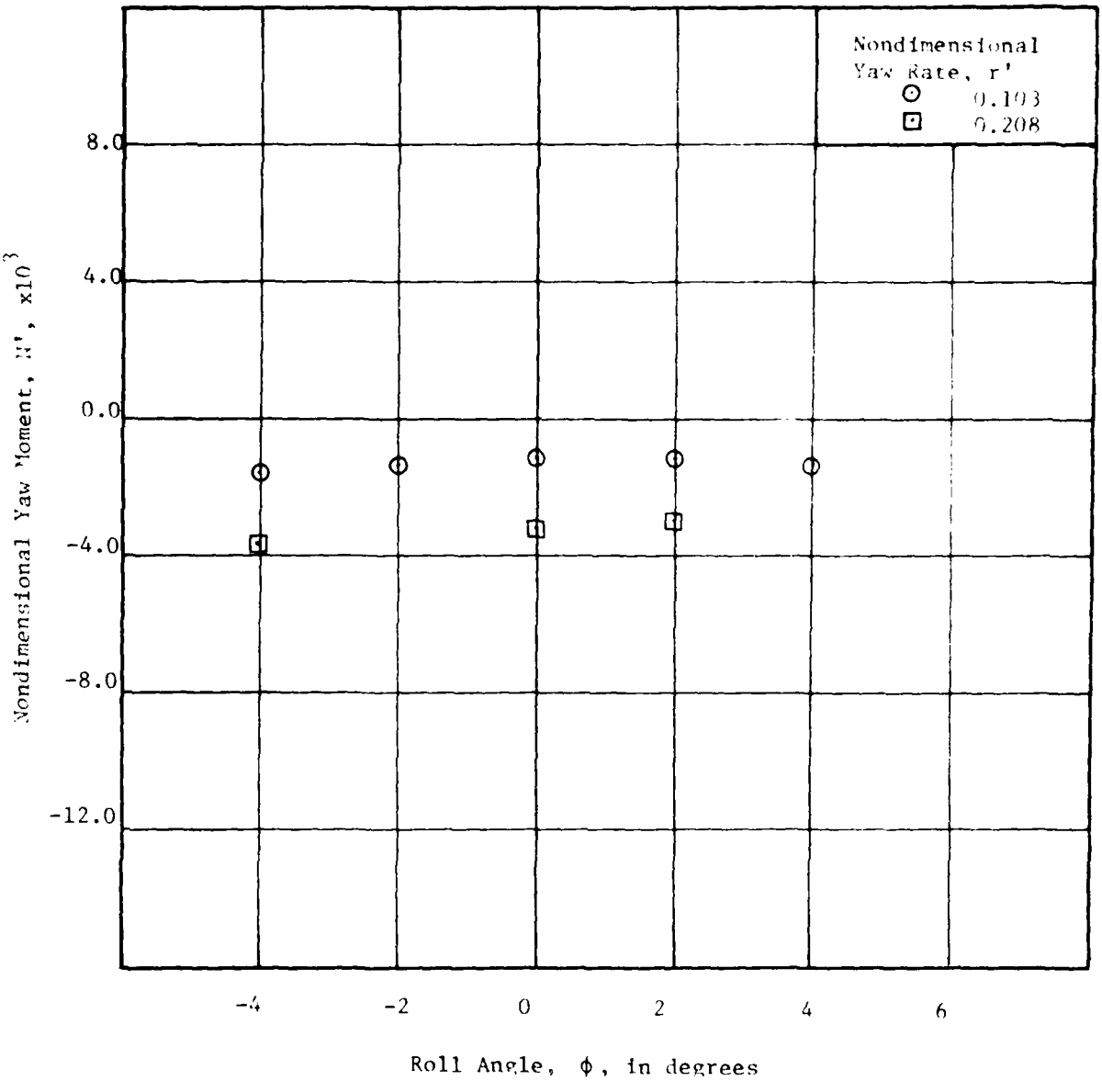

Figure 16 - Variation of Nondimensional Yaw Moment with Roll Angle for Two Nondimensional Yaw Rates at a Full Scale Speed of 20 Knots at Deep Draft

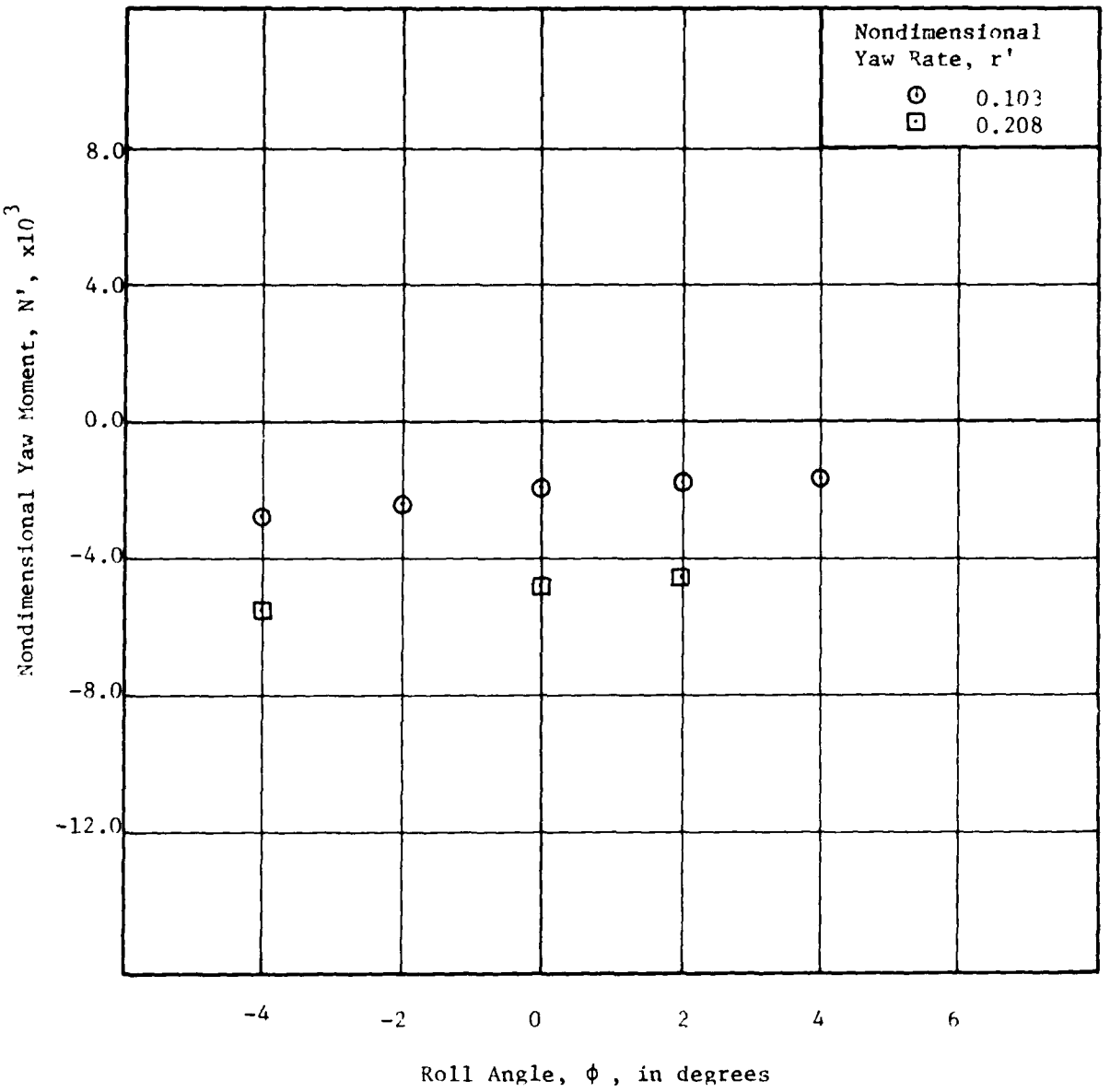

Figure 17 - Variation of Nondimensional Yaw Moment with Roll Angle for Two Nondimensional Yaw Rates at a Full Scale Speed of 25 Knots at Deep Draft

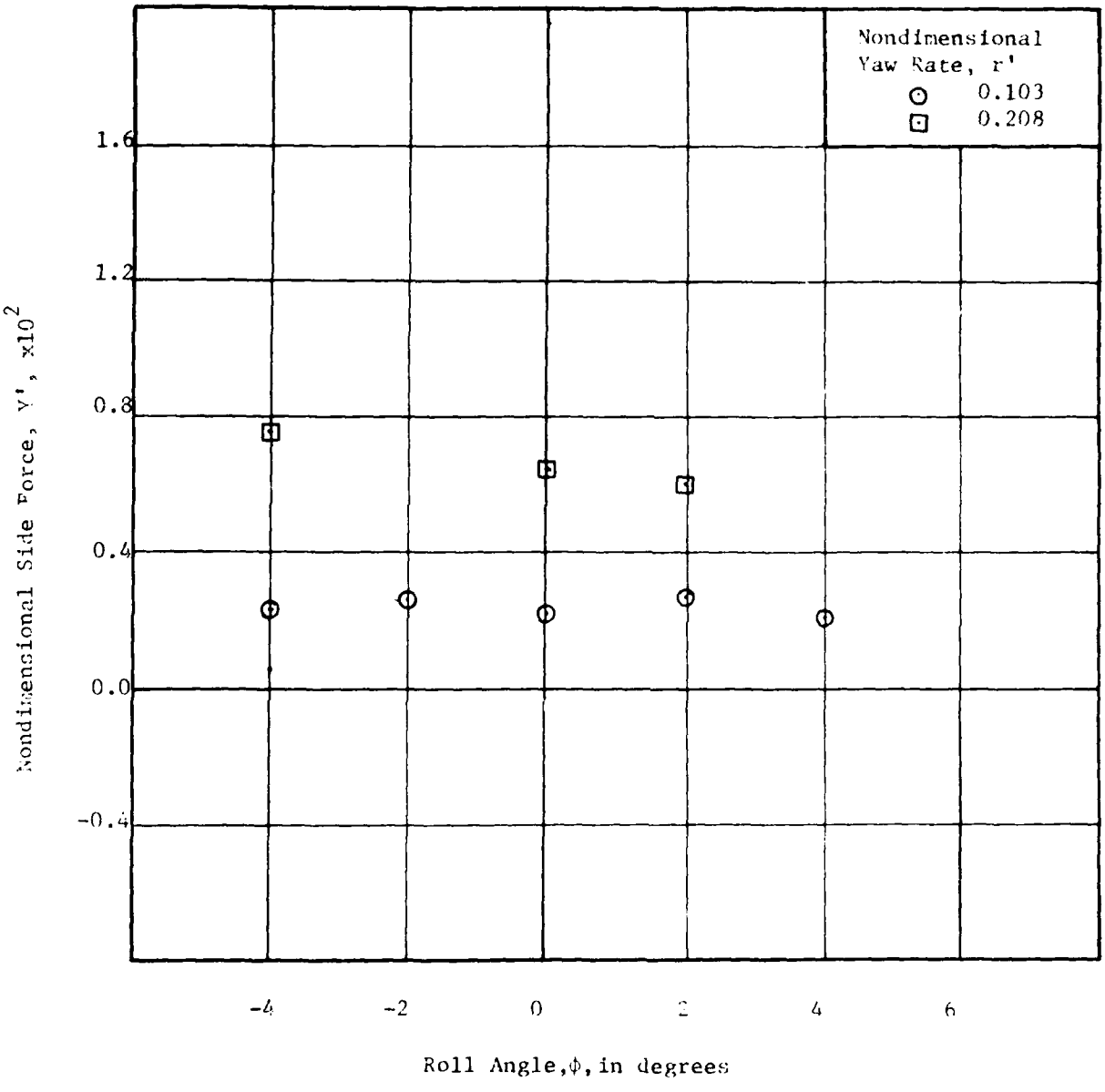

Figure 18- Variation of Nondimensional Side Force with Roll Angle for Two Nondimensional Yaw Rates at a Full Scale Speed of 20 Knots at Deep Draft

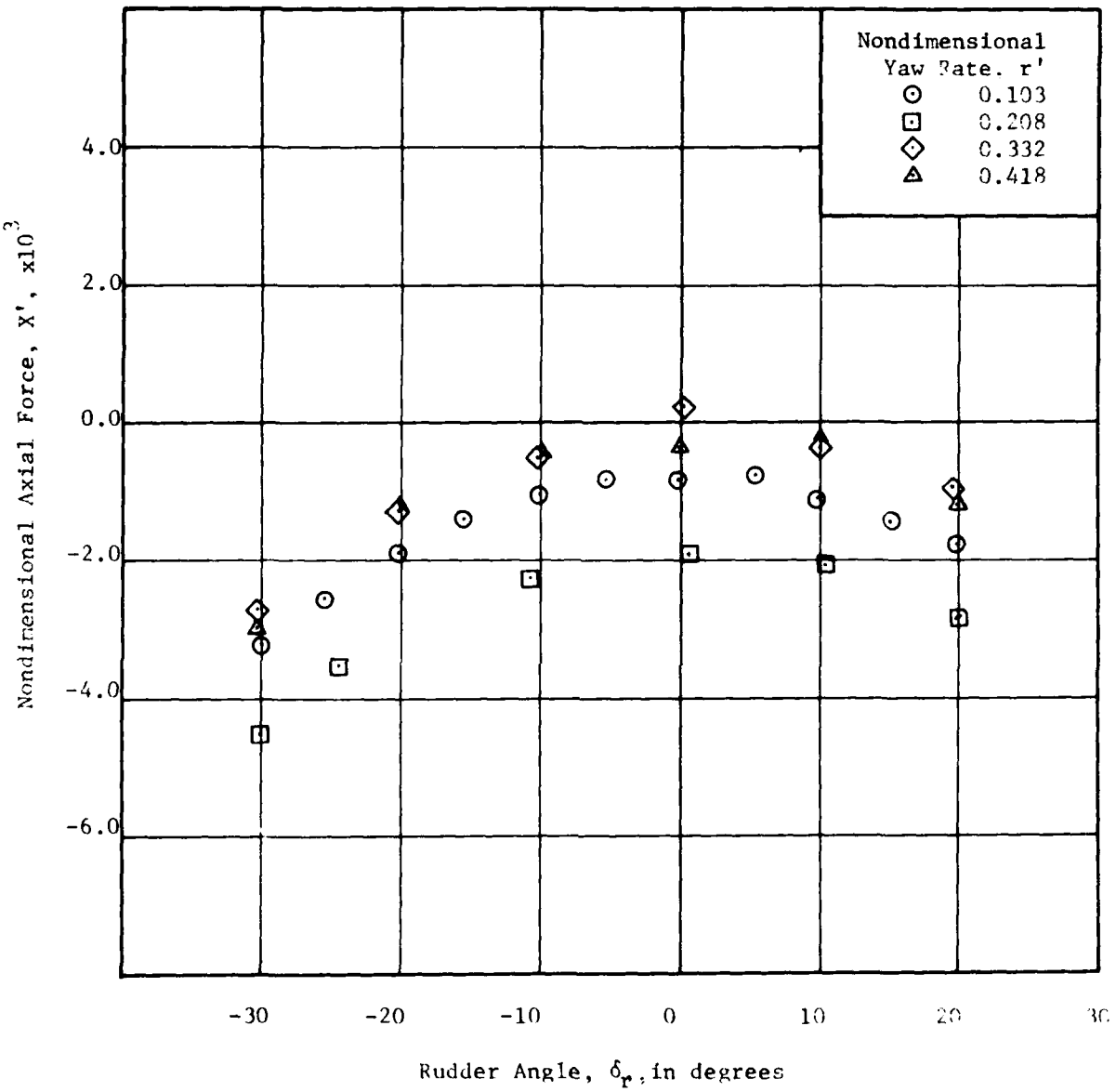

Figure 19- Variation of Nondimensional Axial Force with Rudder Angle for a Series of Nondimensional Yaw Rates at a Full Scale Speed of 15 Knots at Deep Draft

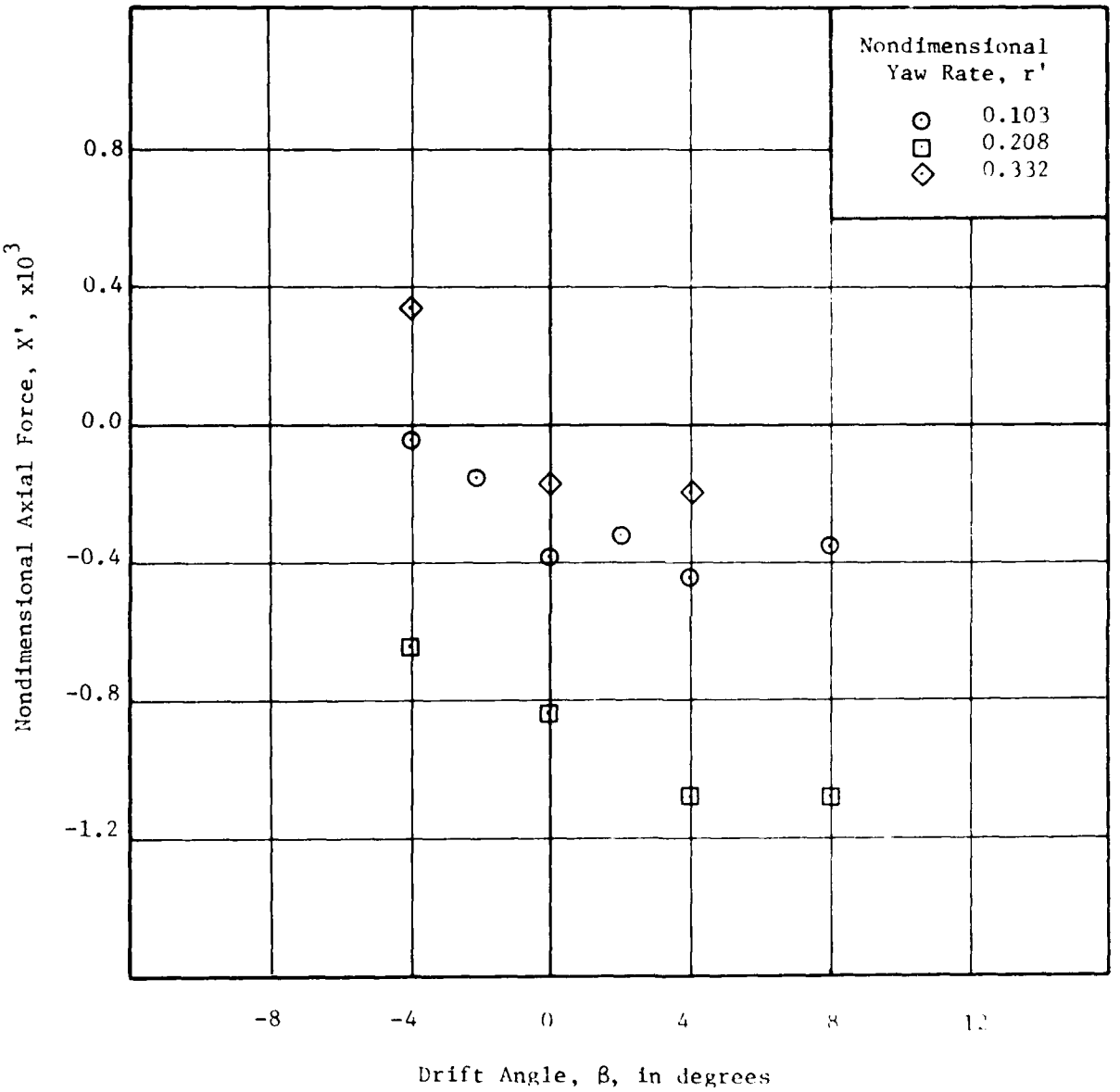

Figure 20 - Variation of Nondimensional Axial Force with Drift Angle for a Series of Yaw Rates at a Full Scale Speed of 25 Knots at Design Draft

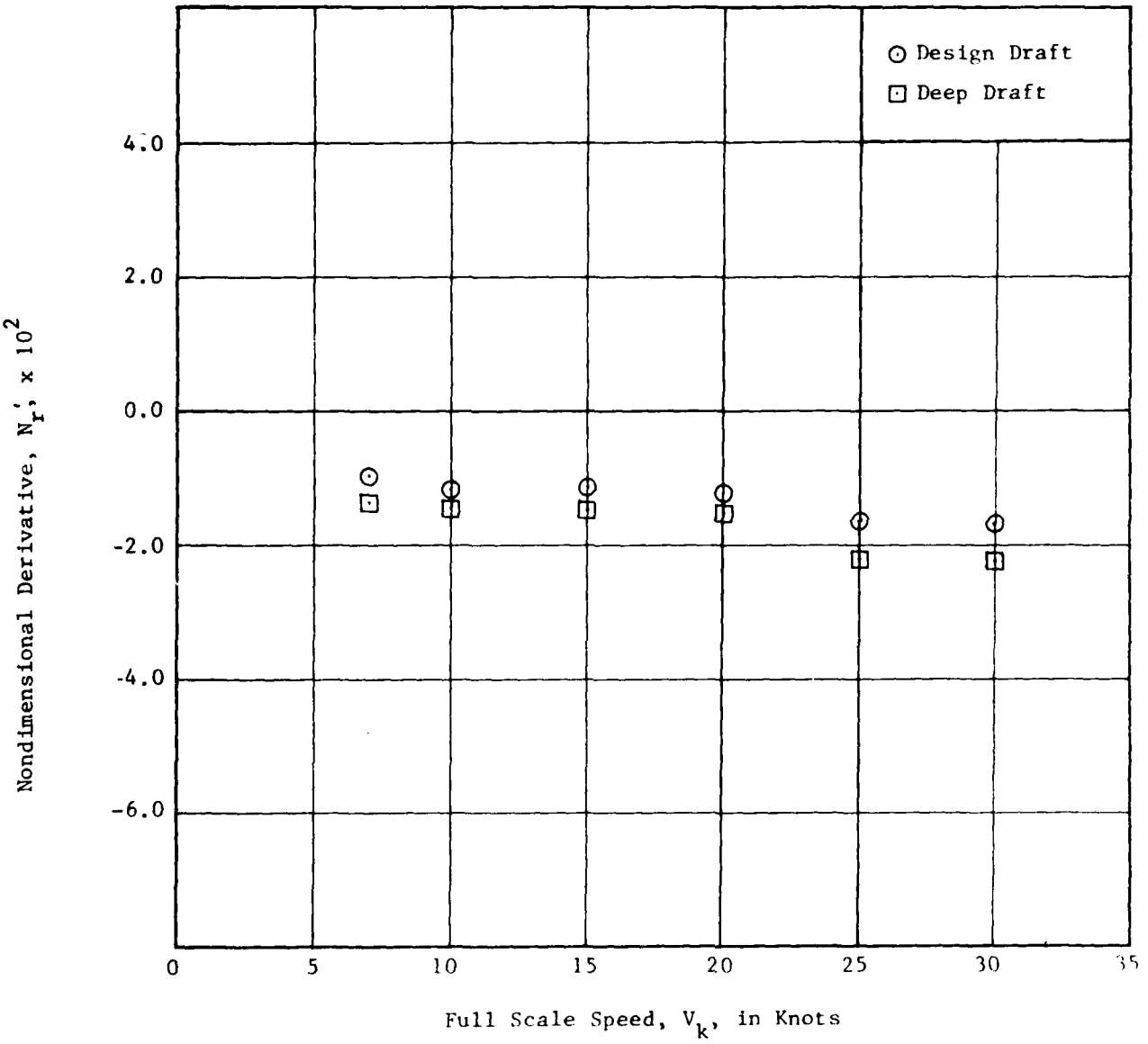

Figure 21- Variation of Nondimensional Derivative, N_r', with Full Scale Speed for Two Draft Configurations

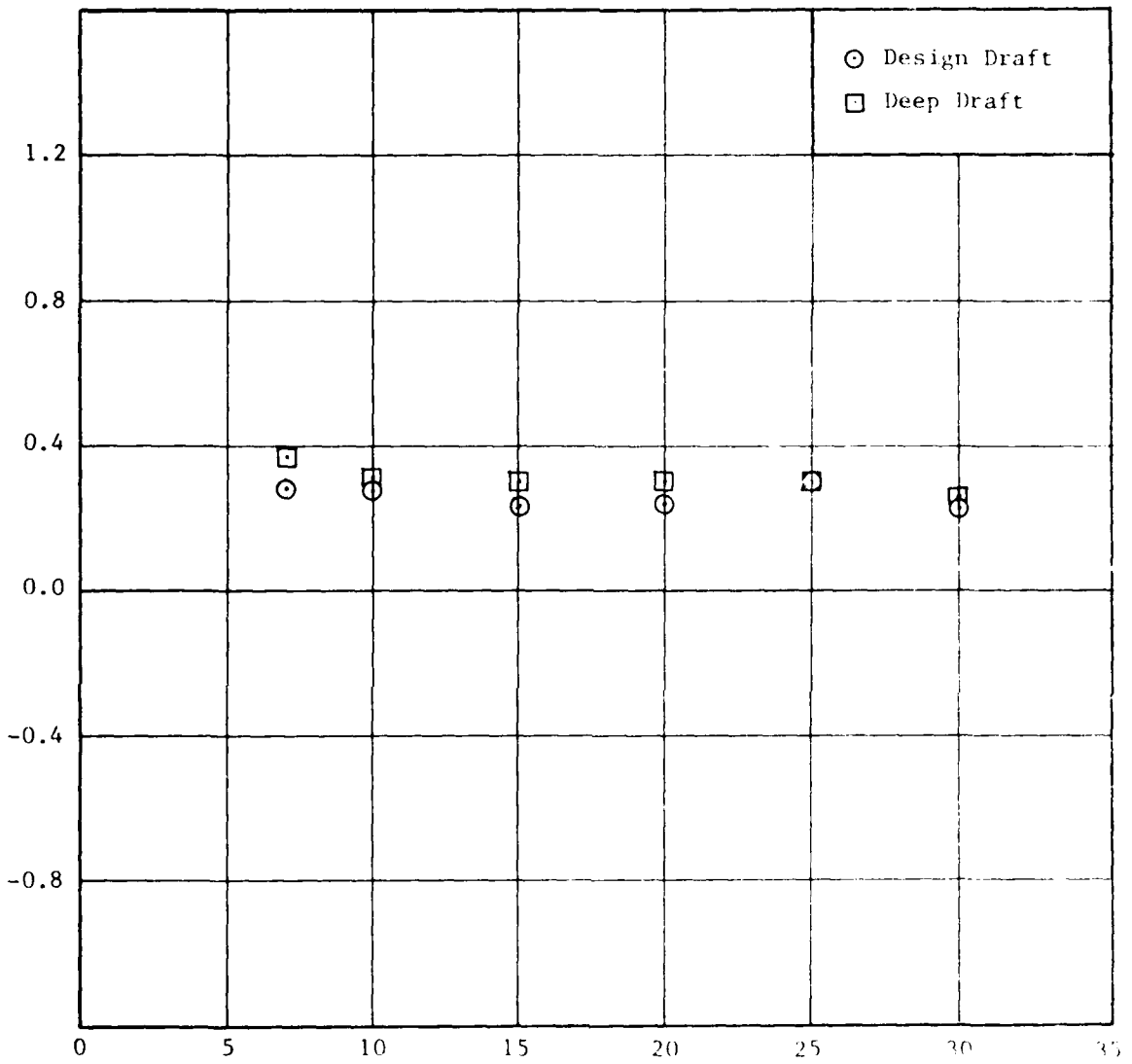

Figure 22- Variation of Nondimensional Derivative, Y_r', with Full Scale Speed for Two Draft Configurations

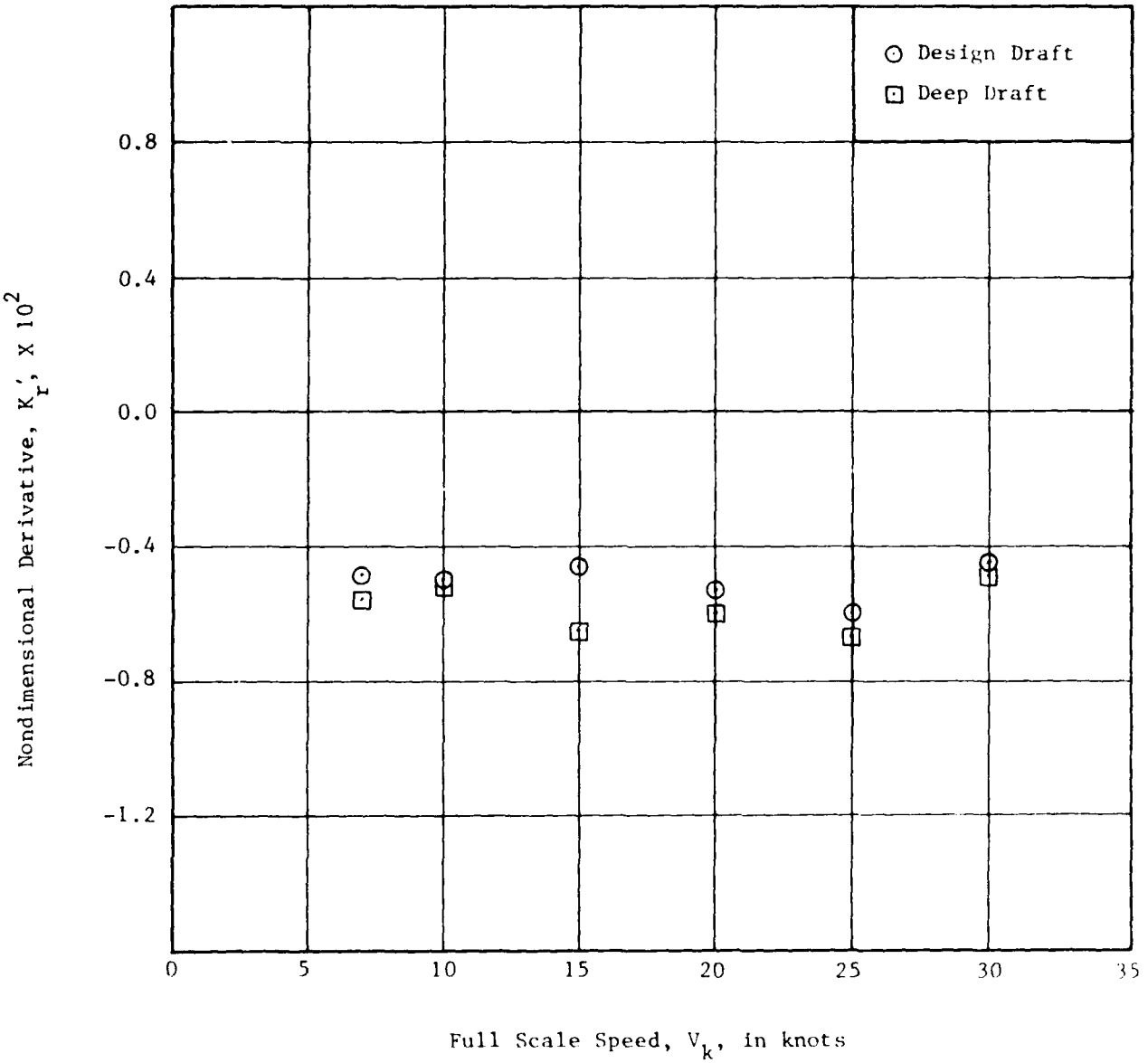

Figure 23 - Variation of Nondimensional Derivative, K_r', with Full Scale Speed for Two Draft Configurations

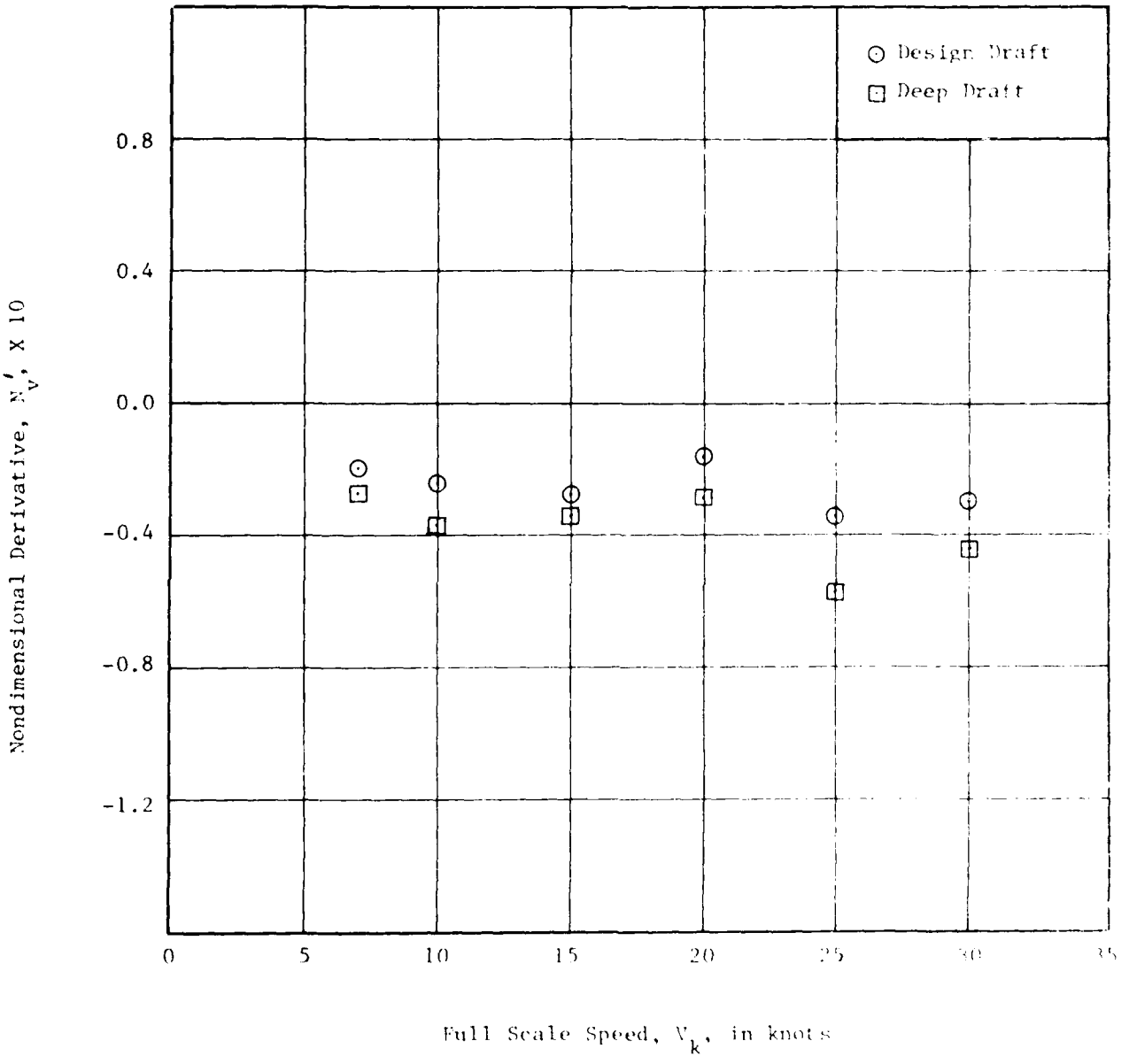

Figure 24 - Variation of Nondimensional Derivative, N_v', with Full Scale Speed for Two Draft Configurations

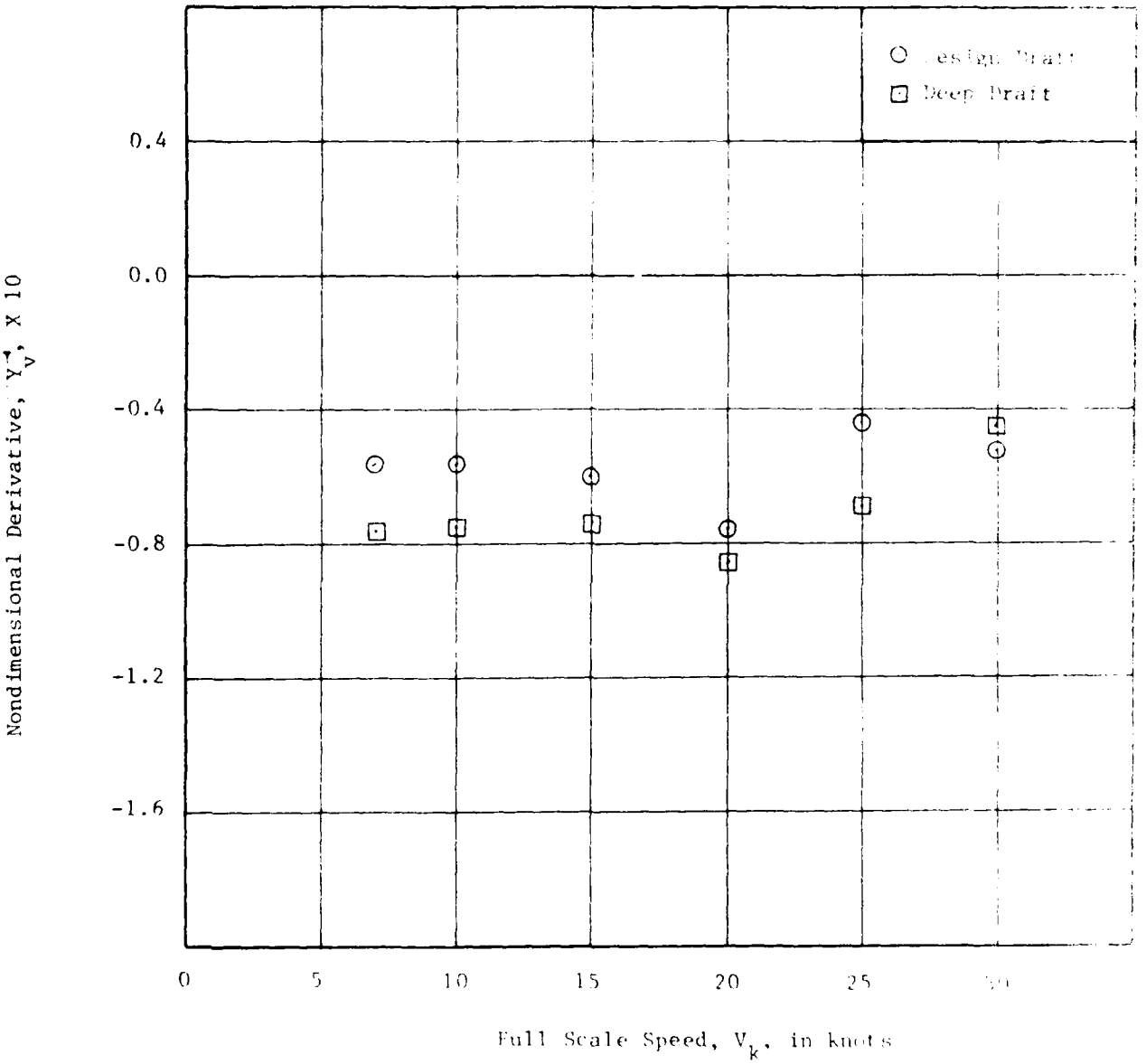

Figure 25 - Variation of Nondimensional Derivative, Y'_v, with Full Scale Speed for Two Draft Configurations

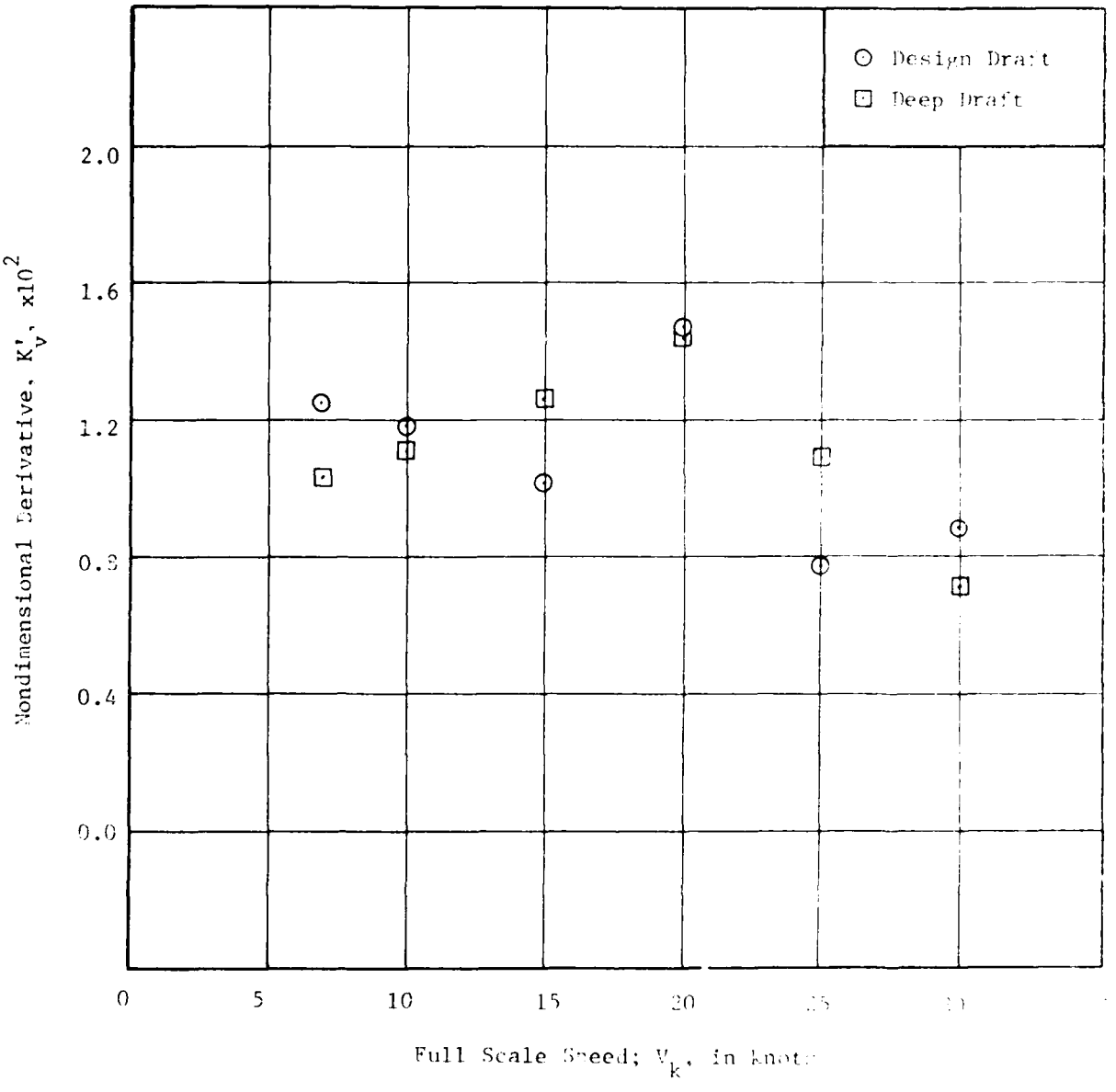

Figure 26- Variation of Nondimensional Derivative, K'_v, with Full Scale Speed for Two Draft Configurations

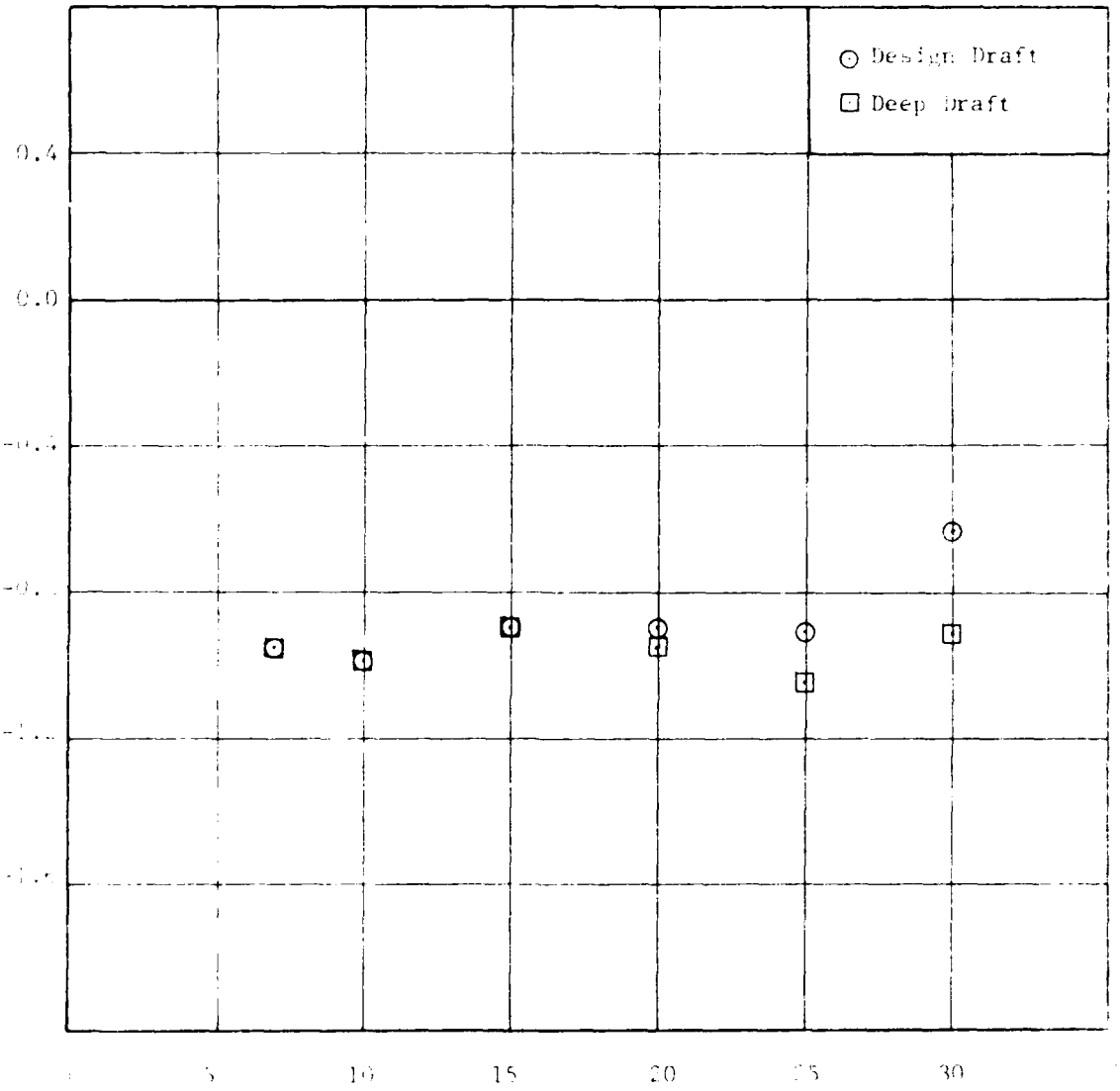

Figure [illegible] Variation of Nondimensional Derivative, N'_{ζ_2}, with Full Scale Speed for Two Draft Configurations

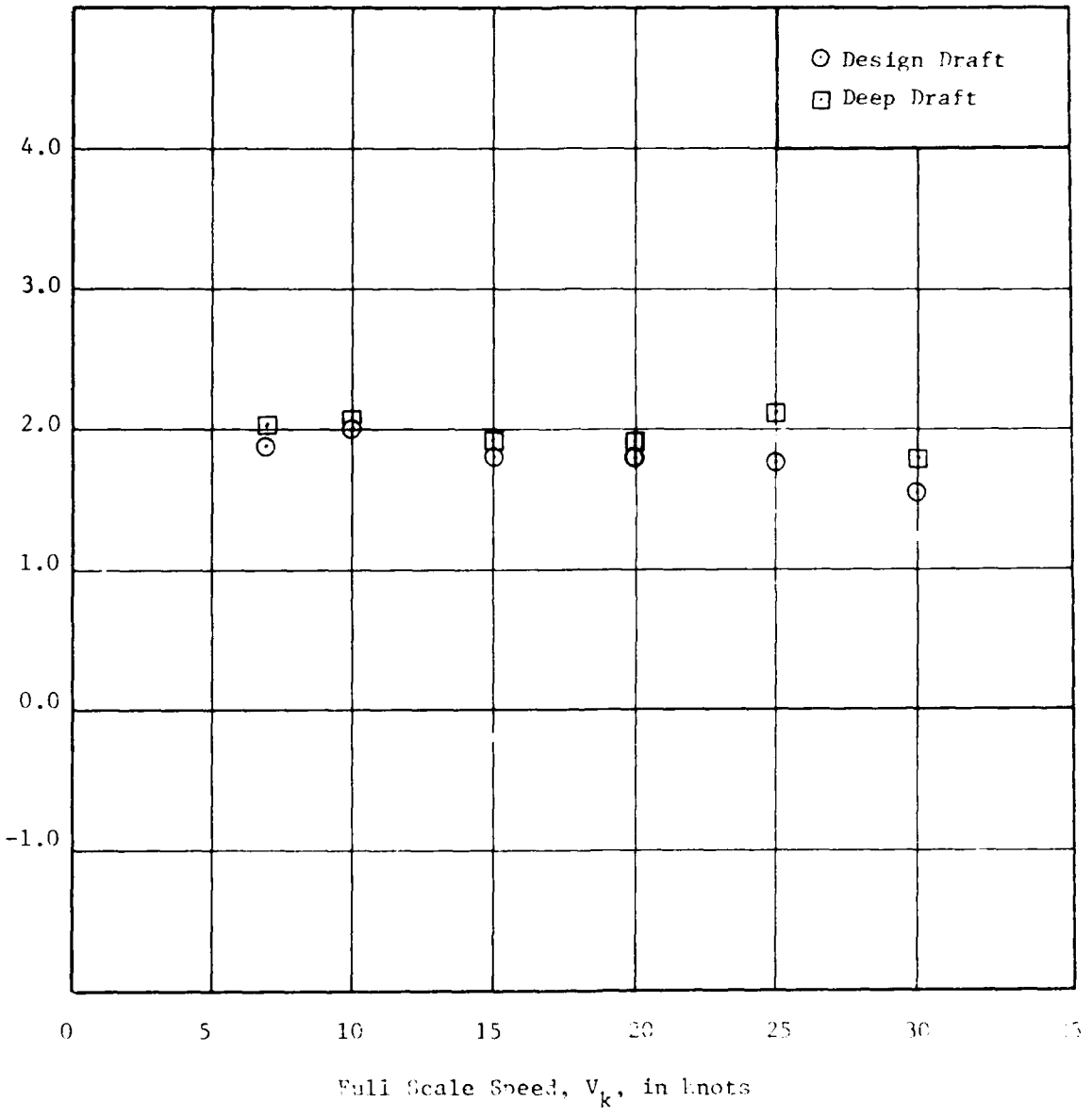

Figure 28- Variation of Nondimensional Derivative, Y'_{δ_r} with Full Scale Speed for Two Craft Configurations

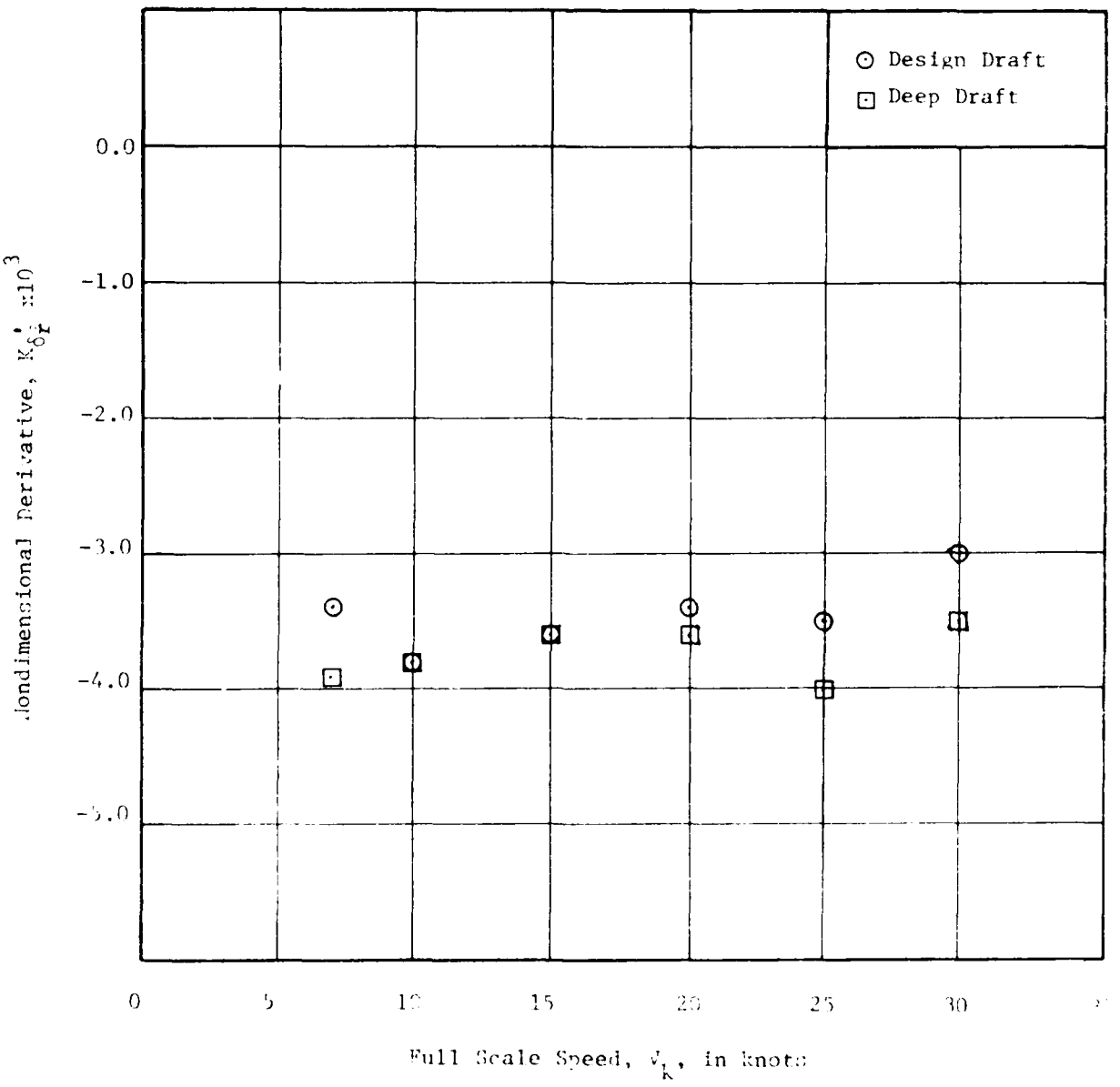

Figure 29 - Variation of Nondimensional Derivative, $K'_{\delta r}$, with Full Scale Speed for Two Draft Configurations

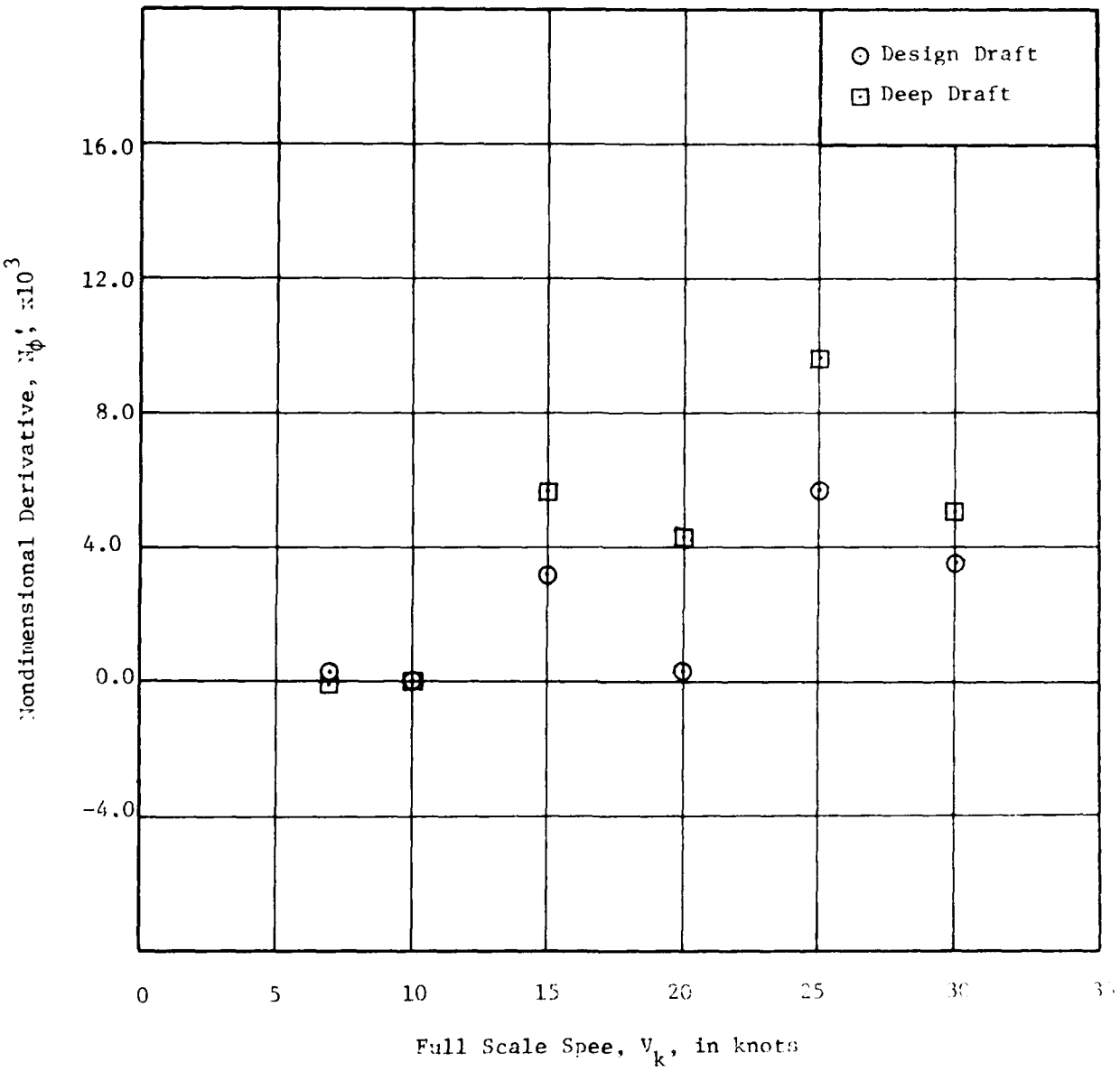

Figure 30 - Variation of Nondimensional Derivative, N_ϕ', with Full Scale Speed for Two Draft Configurations

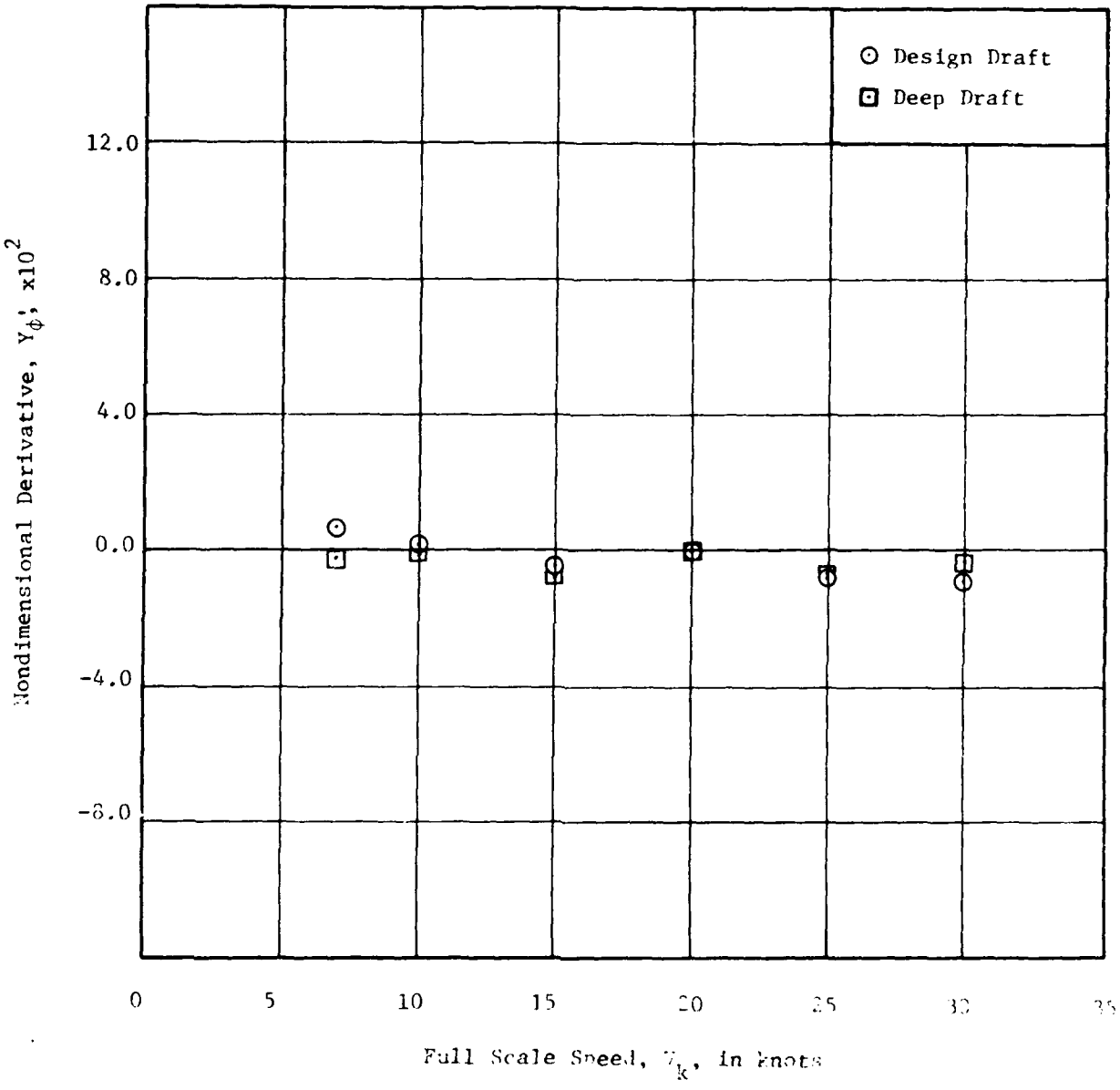

Figure 31- Variation of Nondimensional Derivative, Y_ϕ', with Full Scale Speed for Two Draft Configurations

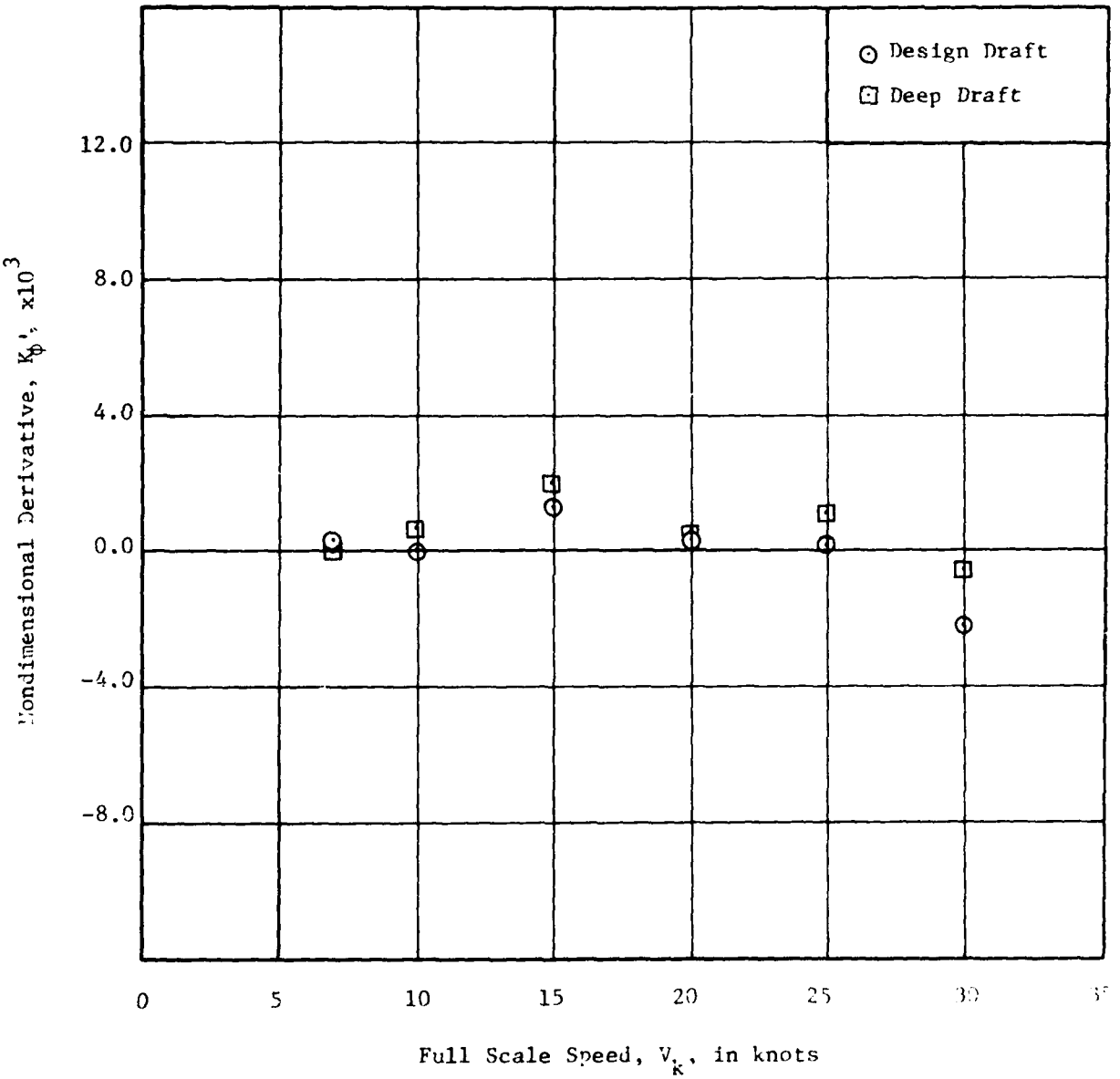

Figure 32- Variation of Nondimensional Derivative, K_ϕ', with Full Scale Speed for Two Draft Configuration

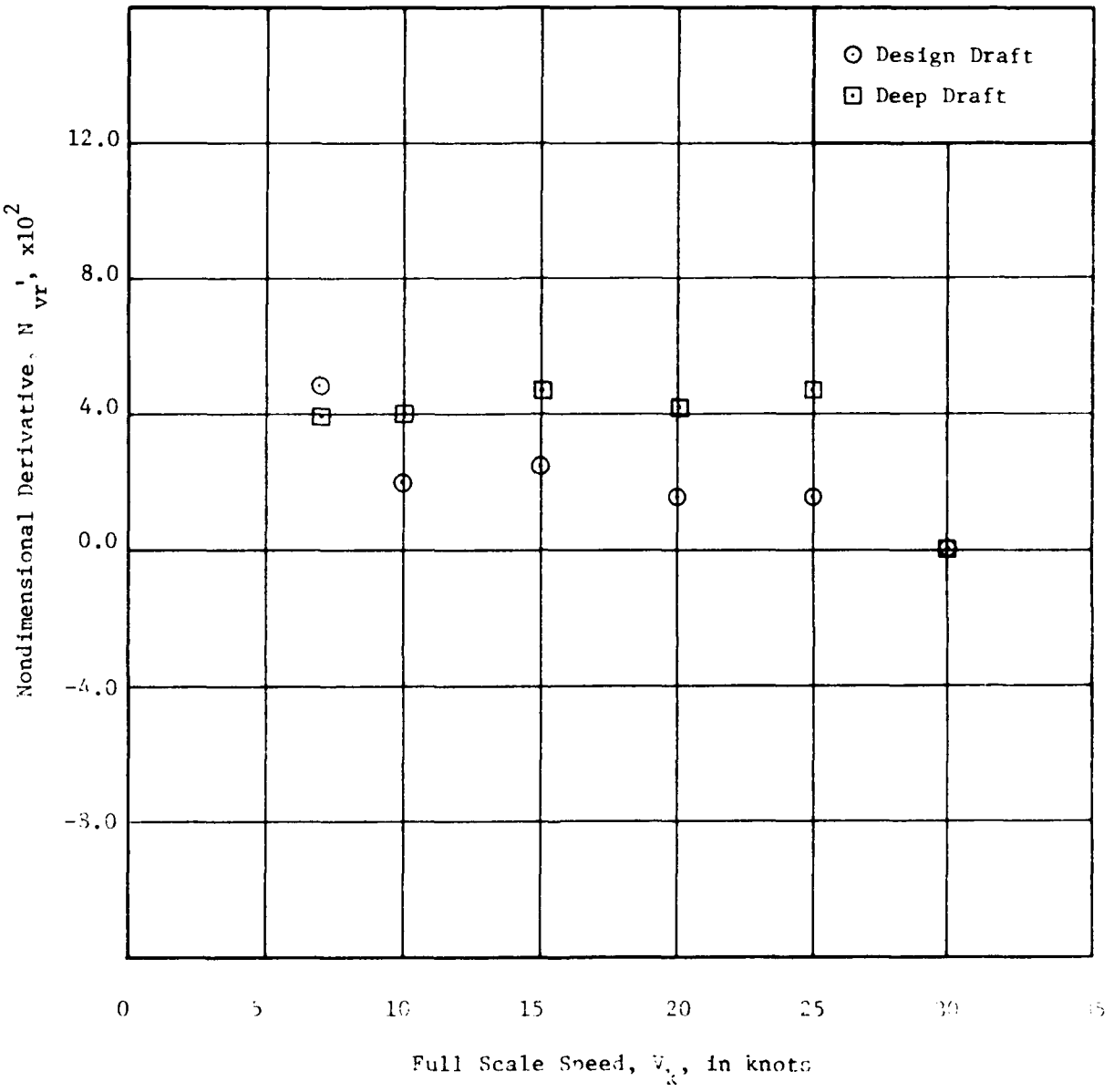

Figure 33 - Variation of Nondimensional Derivative, N'_{vr}, with Full Scale Speed for Two Draft Configurations

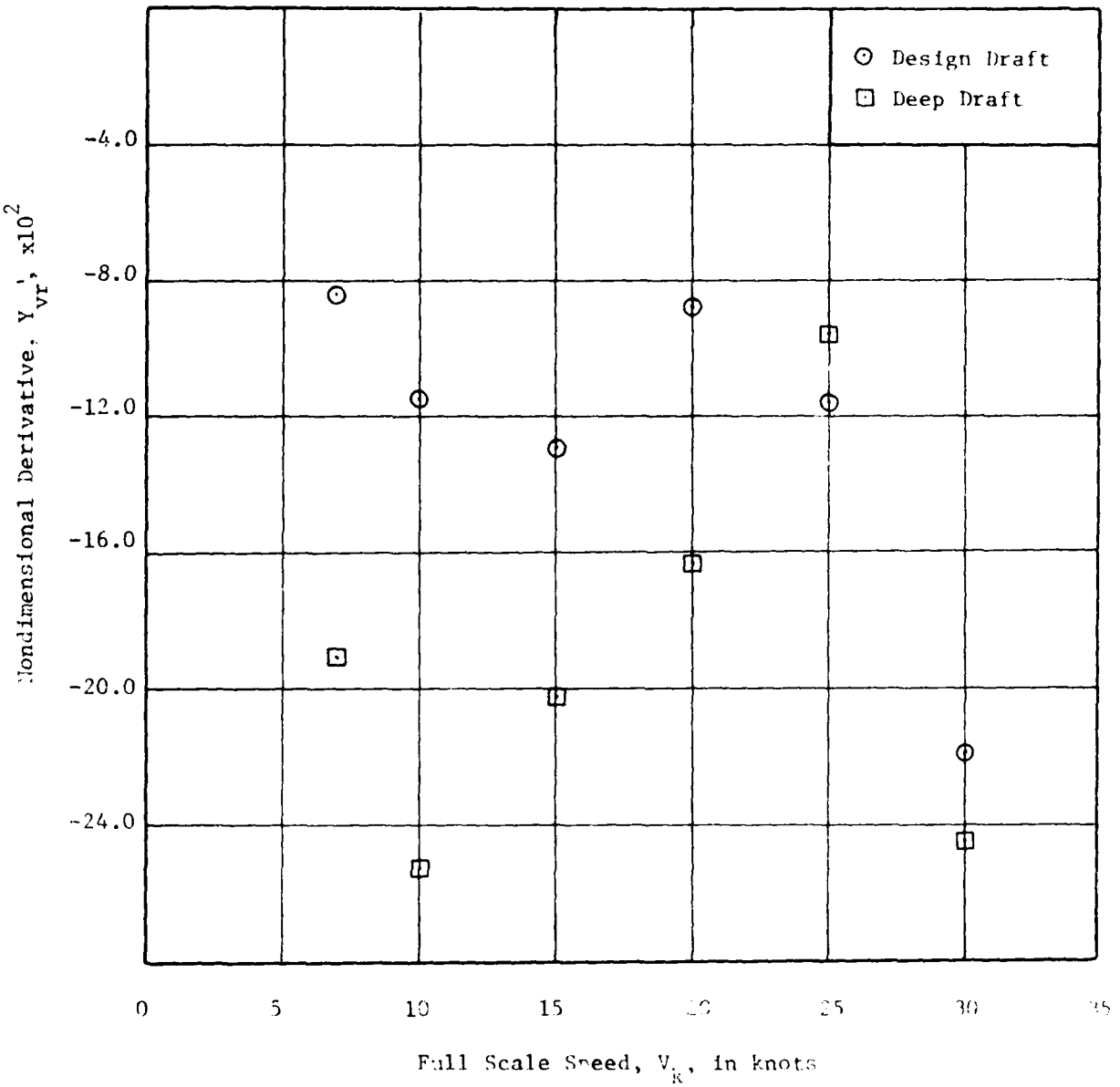

Figure 34 - Variation of Nondimensional Derivative, Y'_{vr}, with Full Scale Speed for Two Draft Configurations

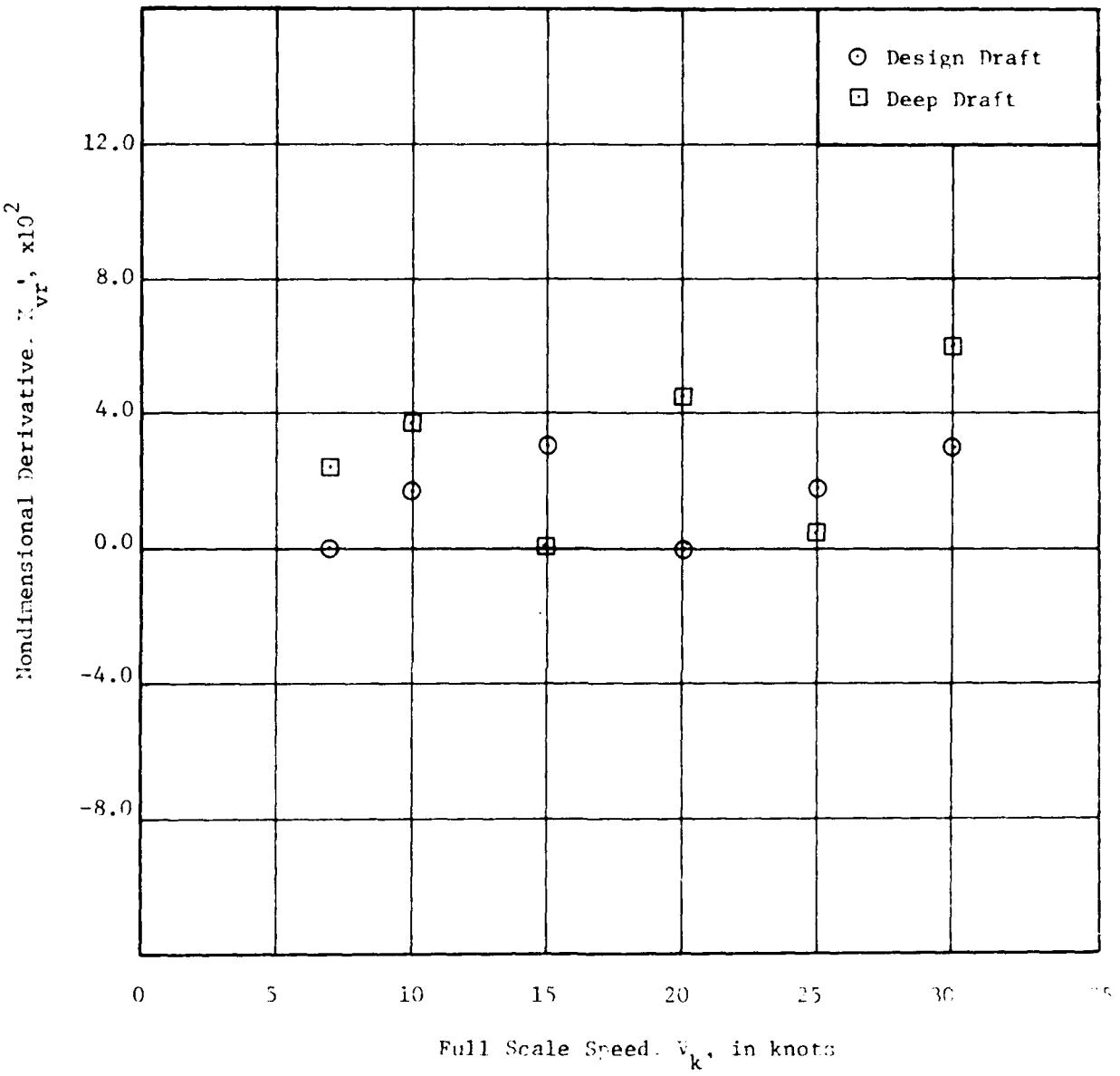

Figure 35 - Variation of Nondimensional Derivative, N'_{vr}, with Full Scale Speed for Two Draft Configurations

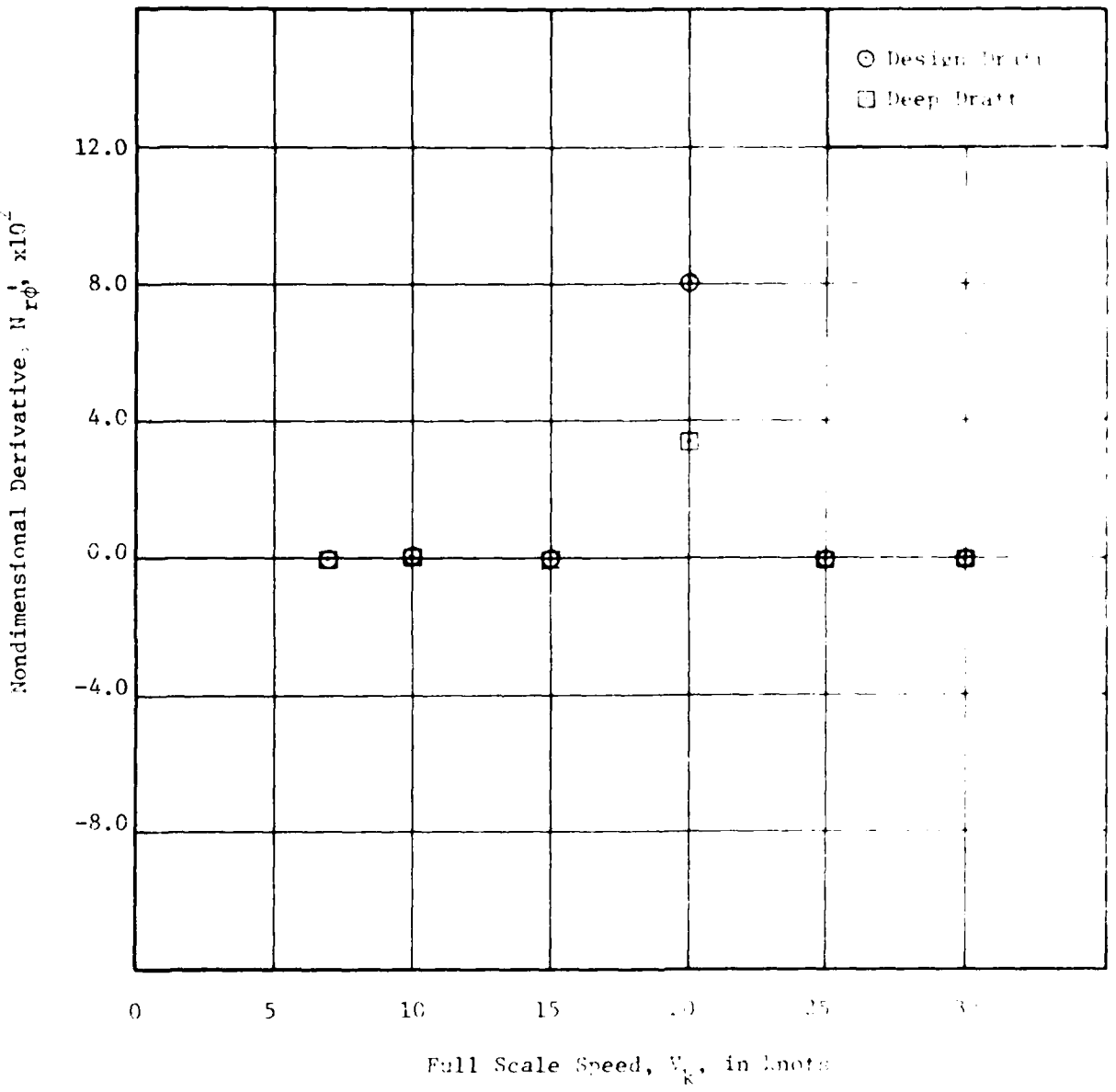

Figure 36 - Variation of Nondimensional Derivative, $N'_{r\phi}$, with Full Scale Speed for Two Draft Configurations

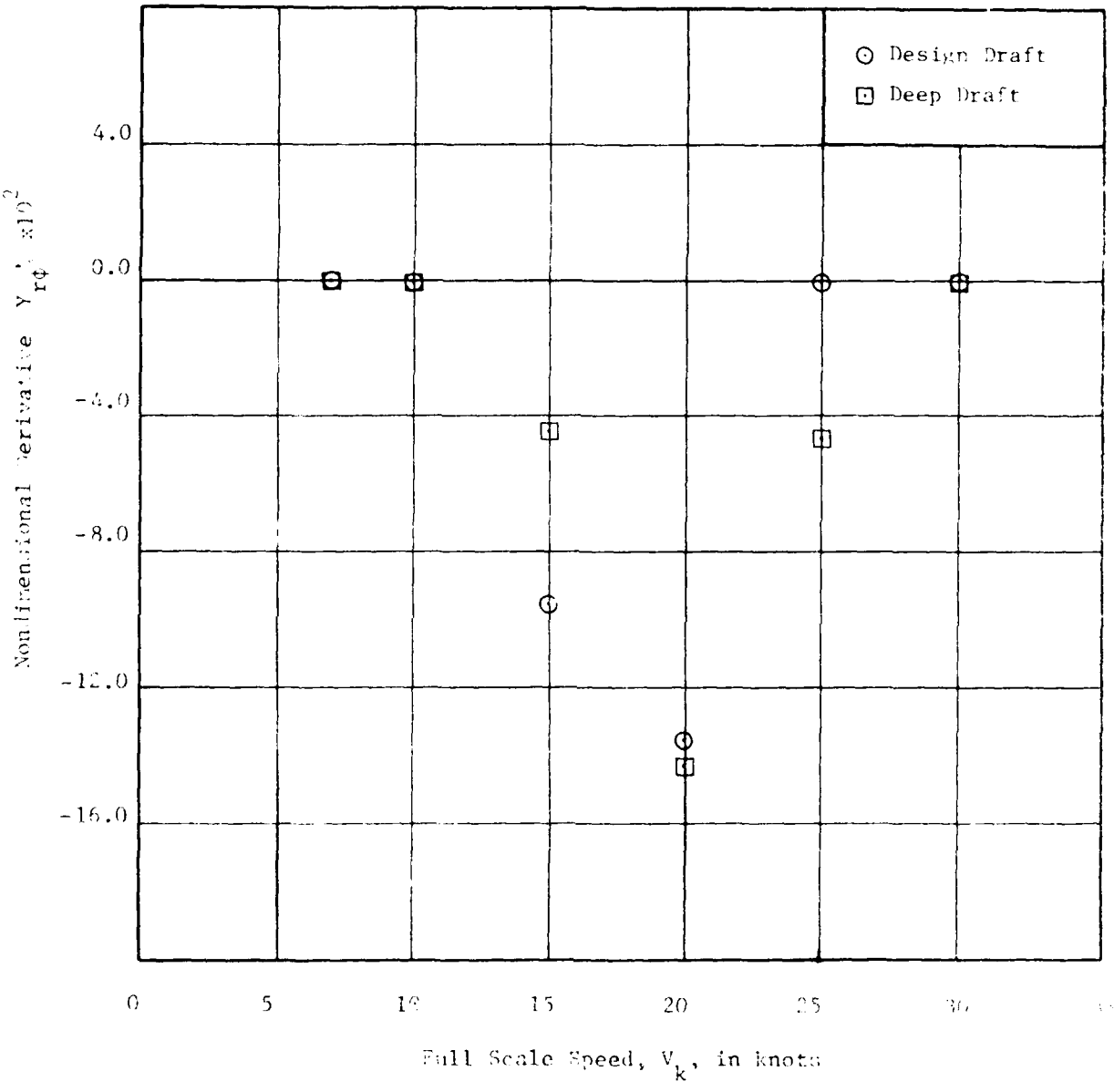

Figure 37- Variation of Nondimensional Derivative, $Y_{r\phi}$, with Full Scale Speed for Two Draft Configurations

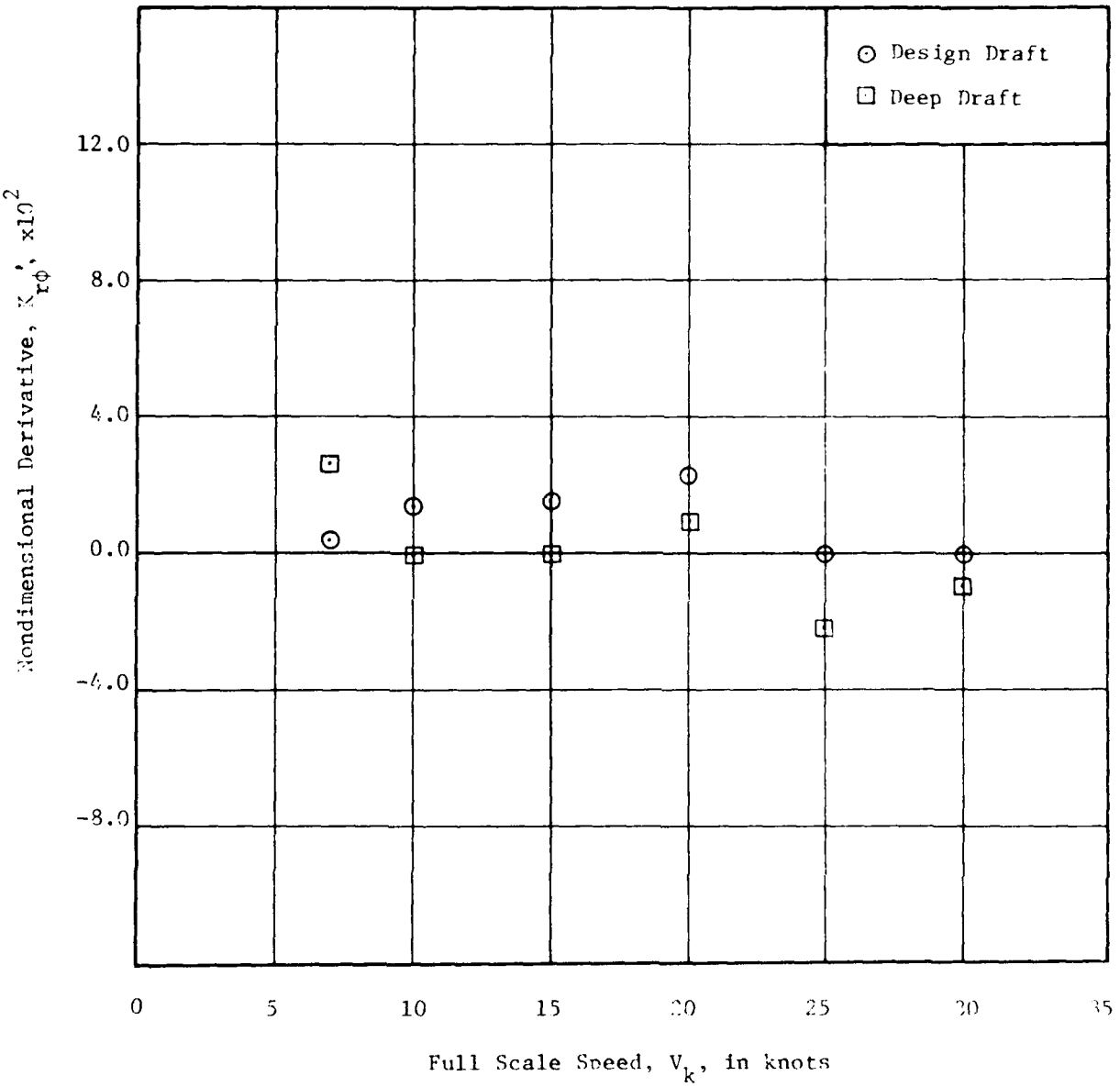

Figure 38 - Variation of Nondimensional Derivative, $K_{r\phi}'$, with Full Scale Speed for Two Draft Configurations

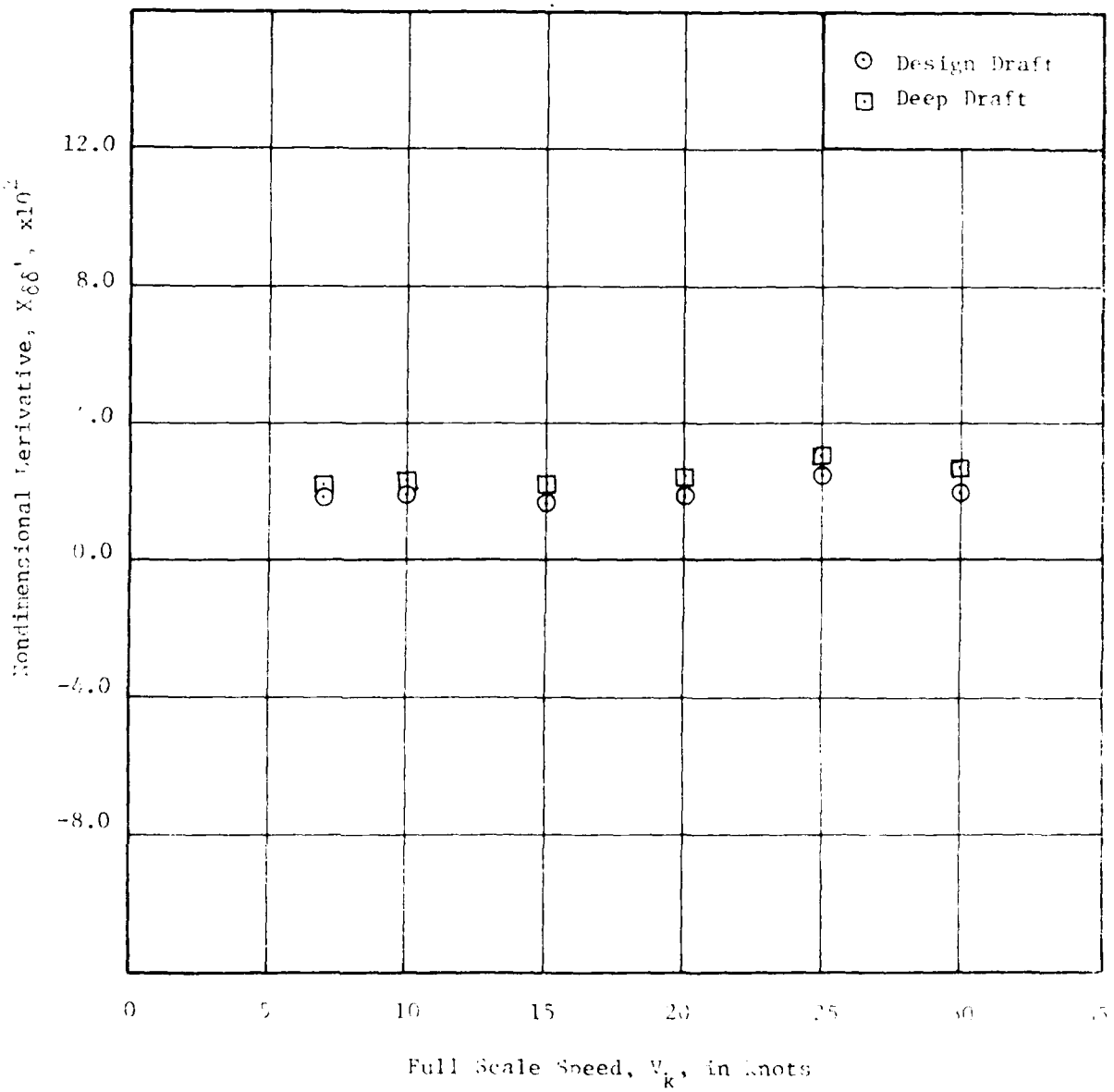

Figure 35 - Variation of Nondimensional Derivative, $Y_{\delta\delta}'$, with Full Scale Speed for Two Draft Configurations

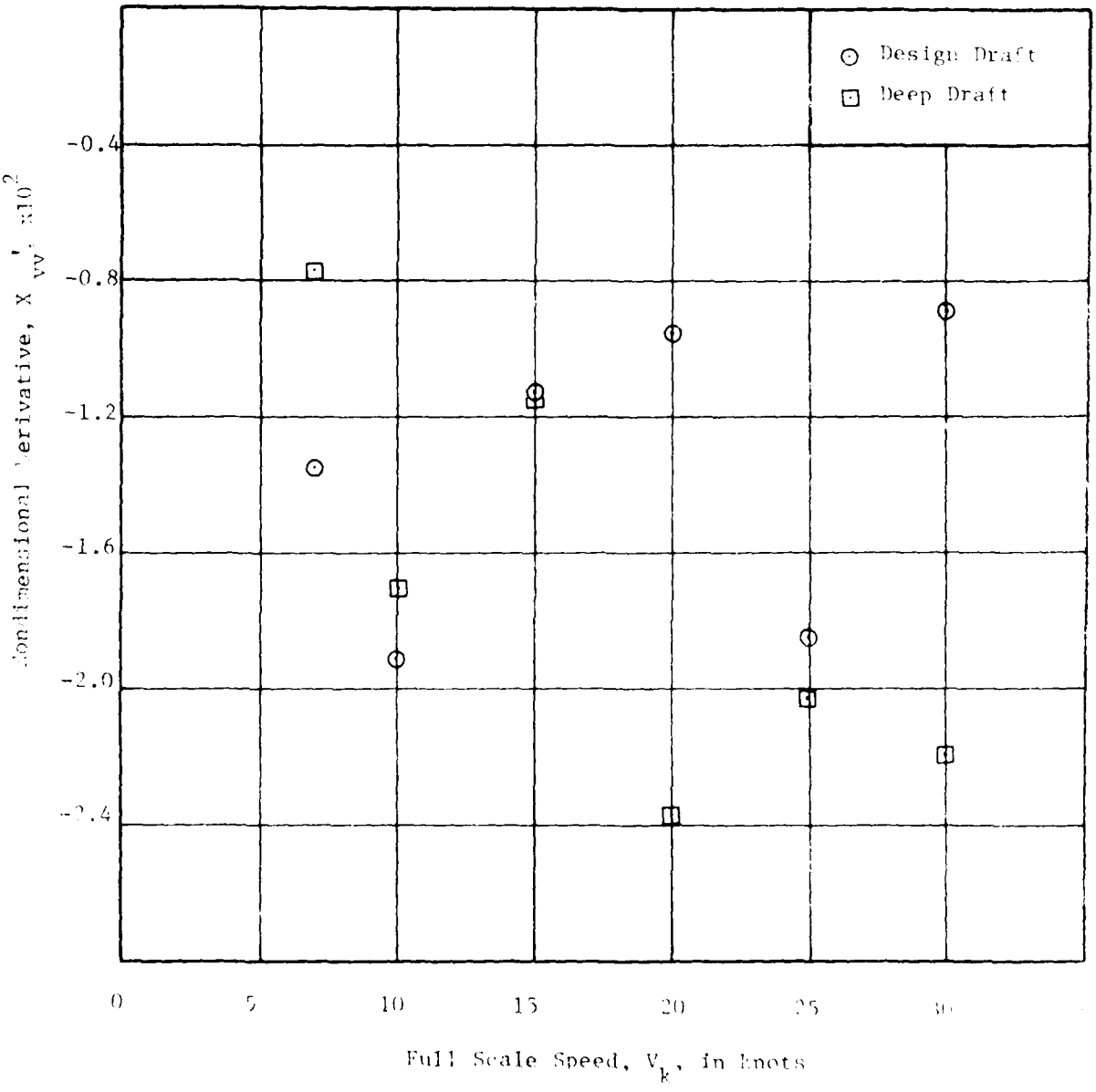

Figure 46- Variation of Nondimensional Derivative, X'_{vv}, with Full Scale Speed for Two Draft Configurations

DTNSRDC ISSUES THREE TYPES OF REPORTS

1 DTNSRDC REPORTS, A FORMAL SERIES, CONTAIN INFORMATION OF PERMANENT TECHNICAL VALUE. THEY CARRY A CONSECUTIVE NUMERICAL IDENTIFICATION REGARDLESS OF THEIR CLASSIFICATION OR THE ORIGINATING DEPARTMENT.

2 DEPARTMENTAL REPORTS, A SEMIFORMAL SERIES, CONTAIN INFORMATION OF A PRELIMINARY, TEMPORARY, OR PROPRIETARY NATURE OR OF LIMITED INTEREST OR SIGNIFICANCE. THEY CARRY A DEPARTMENTAL ALPHANUMERICAL IDENTIFICATION.

3 TECHNICAL MEMORANDA, AN INFORMAL SERIES, CONTAIN TECHNICAL DOCUMENTATION OF LIMITED USE AND INTEREST. THEY ARE PRIMARILY WORKING PAPERS INTENDED FOR INTERNAL USE. THEY CARRY AN IDENTIFYING NUMBER WHICH INDICATES THEIR TYPE AND THE NUMERICAL CODE OF THE ORIGINATING DEPARTMENT. ANY DISTRIBUTION OUTSIDE DTNSRDC MUST BE APPROVED BY THE HEAD OF THE ORIGINATING DEPARTMENT ON A CASE-BY-CASE BASIS.

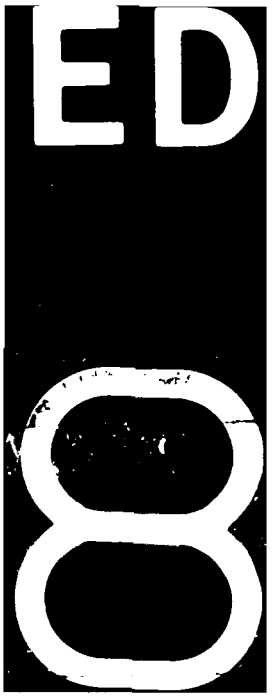
ED
8